On the dynamics of multi-species Ricker models admitting a carrying simplex

Mats Gyllenberg[a], Jifa Jiang[b], Lei Niu[a], Ping Yan[a,c]

[a] *Department of Mathematics and Statistics, University of Helsinki, Helsinki FI-00014, Finland*
[b] *Mathematics and Science College, Shanghai Normal University, Shanghai 200234, China*
[c] *School of Sciences, Zhejiang A & F University, Hangzhou 311300, China*

Abstract

We study the dynamics of the multi-species Ricker model given by the map $T : \mathbb{R}^n_+ \to \mathbb{R}^n_+$ defined by

$$T_i(x) = x_i \exp(\nu_i(1 - \sum_{j=1}^{n} \mu_{ij} x_j)),\ \nu_i, \mu_{ij} > 0, i, j = 1, \cdots, n.$$

It is known that under mild conditions (for small ν_i), T admits a carrying simplex Σ, which is a globally attracting invariant hypersurface of codimension one. We define an equivalence relation relative to local stability of fixed points on the boundary of Σ on the space of all 3D Ricker models admitting a carrying simplex. There are a total of 33 stable equivalence classes. We list them in terms of simple inequalities on the parameters ν_i and μ_{ij}, and draw the phase portrait on Σ of each class. Classes $1 - 25$ and 33 have trivial dynamics, i.e. every orbit converges to some fixed point, and in particular, the unique positive fixed point in class 33 is globally asymptotically stable. Within each of classes 26 to 31, there exist Neimark-Sacker bifurcations, while in class 32 Neimark-Sacker bifurcations cannot occur. Class 29 can admit Chenciner bifurcations, so two isolated closed invariant curves can coexist on the carrying simplex in this class. Each map in class 27 admits a heteroclinic cycle, i.e. a cyclic arrangement of saddle fixed points and heteroclinic connections. As ν_i increases the carrying simplex will break, and chaos can occur for large ν_i. We also numerically show that the 4D Ricker map can admit a carrying simplex containing a chaotic attractor, which is found in competitive mappings for the first time.

Email addresses: `mats.gyllenberg@helsinki.fi` (Mats Gyllenberg), `jiangjf@shnu.edu.cn` (Jifa Jiang), `lei.niu@helsinki.fi` (Lei Niu), `ping.yan@helsinki.fi` (Ping Yan)

This article has been accepted for publication in Journal of Difference Equations and Applications, published by Taylor & Francis with DOI: 10.1080/10236198.2019.1663182.

Keywords: Carrying simplex, Ricker model, classification, Neimark-Sacker bifurcation, Chenciner bifurcation, closed invariant curve, quasiperiodic curve, heteroclinic cycle, chaos

1. Introduction

By Hirsch's carrying simplex theory [24], it is known that every strongly competitive and dissipative system of Kolmogorov ODEs for which the origin is a repeller possesses a globally attracting invariant hypersurface Σ of codimension one, such that every nontrivial orbit in the nonnegative cone $\mathbb{R}^n_+$ is asymptotic to one in Σ. This result implies that n-dimensional strongly competitive continuous-time systems behave like general $(n-1)$-dimensional systems, and hence the Poincaré-Bendixson theorem holds for the 3-dimensional case. Based on this remarkable theory, many researchers have obtained a lot of results on nontrivial dynamics for 3-dimensional continuous-time competitive systems, including the existence and multiplicity of limit cycles [21, 22, 23, 28, 35, 39, 57, 58, 62]; the existence of centers and heteroclinic cycles [8, 35, 62]; and ruling out periodic orbits [8, 35, 54, 62]. Moreover, the readers can consult [2, 3, 5, 29, 30, 42, 61, 60, 59] for the geometrical properties of carrying simplices and their impact on the dynamics.

The research on the existence of carrying simplex for discrete-time systems began with Smith's work [52] on the dynamical behavior of the Poincaré map induced by time-periodic competitive Kolmogorov ODEs. Based on the early work of Hirsch [24] and Smith [52], there have been many results on the existence of carrying simplex for competitive mappings; see [56, 11, 25, 49, 4, 34, 33]. In the recent article [33], Jiang and Niu provided a readily checked criterion that guarantees the existence of carrying simplex for the continuously differentiable map $T : \mathbb{R}^n_+ \to \mathbb{R}^n_+$ of the type

$$T(x) = (T_1(x), \cdots, T_n(x)) = (x_1G_1(x), \cdots, x_nG_n(x)), \qquad (1)$$

where $G_i(x) > 0$, $i = 1, \cdots, n$, for all $x \in \mathbb{R}^n_+$. They applied this criterion to show that all maps in a large family of continuously differentiable competitive maps have a carrying simplex. Their result enriches the existing literature on discrete-time competitive dynamical systems with a carrying simplex. For competitive maps given in (1) that are not necessarily differentiable, see, e.g. [25, 49]. We refer the readers to [33] for a review of the development of carrying simplex theory for competitive mappings and the comparison among different criteria.

The importance of the existence of carrying simplex Σ stems from the fact that Σ captures the relevant long-term dynamics. It contains all non-trivial fixed points, periodic orbits, invariant closed curves and heteroclinic cycles, etc. In order to analyze the global dynamics of such discrete-time systems, it suffices to investigate the dynamics on Σ. However, compared with the continuous-time competitive systems, the research on discrete-time competitive systems via carrying simplices is much less. In [49] Ruiz-Herrera provided an exclusion criterion for discrete-time competitive models of two or three species via carrying simplices. Jiang and Niu [32] deduced an index formula on the sum of the indices of all fixed points on Σ for the three-dimensional map T of type (1):

$$\sum_{\theta\in\mathcal{E}_v}\mathscr{I}(\theta,T)+2\sum_{\theta\in\mathcal{E}_s}\mathscr{I}(\theta,T)+4\sum_{\theta\in\mathcal{E}_p}\mathscr{I}(\theta,T)=1. \tag{2}$$

Here $\mathscr{I}(\theta,T)$ stands for the index of T at the fixed point θ, and $\mathcal{E}_v$, $\mathcal{E}_s$, and $\mathcal{E}_p$ are the sets of nontrivial axial, planar, and positive fixed points, respectively. Based on the index formula (2), an alternative classification for 3-dimensional ($n=3$) Atkinson–Allen models was given in [32] and an alternative classification for 3-dimensional Leslie–Gower models was also given in [33]. Neimark–Sacker bifurcations were investigated within each class of these two types of models. Neimark-Sacker bifurcation is the birth of an invariant closed curve from a fixed point in discrete-time dynamical systems, and either all orbits are periodic, or any orbit is dense on the invariant closed curve. Such an invariant closed curve corresponds to either subharmonic or quasiperiodic solutions in continuous-time systems. In [34], Jiang *et al.* studied the occurrence of heteroclinic cycles via carrying simplices for competitive maps (1) and provided their stability criteria.

In his seminal paper [45], Ricker introduced the discrete-time model

$$x_{n+1}=T(x_n):=x_ne^{r(1-x_n)},\quad n=0,1,2,\dots \tag{3}$$

to describe the time evolution of the density x of a single-species (fish) population. It has been extensively studied, for instance by May and Oster [41] who showed that every orbit converges to the positive fixed point for $r\le 2$, and it exhibits a scenario of chaotic behavior for large values of r.

The model (3) can be extended to the case of N species for instance in the following way assuming competition in the nursery only.

Let x_i be the density of newborn juveniles of species i in the beginning of a season and let $z_i(t)$ be the corresponding densities during the juvenile period. We assume that the juvenile period is short (of length ε) and that the juveniles compete intensively, that is, with large Lotka–Volterra competition coefficients a_{ij}/ε. The dynamics of the juveniles is then given by the following initial value problem:

$$\frac{d}{dt}z_i(t)=-z_i(t)\sum_{j=1}^{n}\frac{a_{ij}}{\varepsilon}z_j(t),\quad 0<t<\varepsilon,\quad z_i(0)=x_i. \tag{4}$$

Integrating (4) one obtains

$$z_i(\varepsilon) = x_i e^{-\sum_{j=1}^{n} \frac{a_{ij}}{\varepsilon} \int_0^{\varepsilon} z_j(t)dt} \tag{5}$$

and letting $\varepsilon \downarrow 0$ in (5) one obtains

$$z_i(0+) = x_i e^{-\sum_{j=1}^{n} a_{ij} x_j}. \tag{6}$$

The quantity in (6) represents those of species i that survived the juvenile period. We now further assume that of these a fraction $\mathcal{F}_i$ survives as adults to the beginning of the next season when they give birth to on average β_i offspring after which they die. Denoting

$$R_0^{(i)} = \beta_i \mathcal{F}_i, \tag{7}$$

$$\nu_i = \ln R_0^{(i)} \tag{8}$$

and

$$\mu_{ij} = \frac{a_{ij}}{\nu_i} \tag{9}$$

one obtains the following map that takes the population densities from the beginning of one season to the beginning of the next one:

$$T_i(x) = x_i \exp(\nu_i(1 - \sum_{j=1}^{n} \mu_{ij} x_j)), \quad i = 1, \cdots, n. \tag{10}$$

The difference equation

$$x_{n+1} = T(x_n) \tag{11}$$

with T given by (10) is called the *multi-species Ricker model* and it is the object of study in this paper. The number $R_0^{(i)}$ is the basic reproduction ratio (expected life time production of offspring) of species i in a virgin environment (in the absence of competition). We shall (slightly sloppily) call ν_i the intrinsic growth rate of species i. If $R_0^{(i)} < 1$ or, equivalently, $\nu_i < 0$, species i will go extinct. We shall therefore assume that $\nu_i > 0$ for $i = 1, 2, \ldots, n$. We shall also assume that the competition coefficients $\mu_{ij} > 0$.

Note that the map (10) is of type (1).

In the case of two competing species ($n = 2$), the map (10) was analyzed in detail by Smith [53], who showed that it has trivial dynamics provided $\nu_1, \nu_2 < 1$. Roeger [46] studied the local dynamics of the positive fixed point and Neimark-Sacker bifurcations for the special 3D maps (10) with $\nu_1 = \nu_2 = \nu_3$ when the species compete in the rock-scissors-paper type. Hofbauer *et al.* [26] studied the long term survival of n species in models governed by (10). Hirsch showed that under mild conditions the Ricker map (10) possesses a carrying simplex by using his criterion (without a proof) provided in [25], which was proved rigorously by Ruiz-Herrera [49]. Roughly speaking, the Ricker map (10) admits a carrying simplex when the growth rates $\nu_i > 0$ are small, that is, when the basic reproduction ratios $R_0^{(i)}$ are only slightly greater than 1.

In this paper, we define an equivalence relation on the space of all 3D Ricker maps (10) which admit a carrying simplex. Two such Ricker maps are said to be equivalent relative to $\partial\Sigma$ (the boundary of Σ) if their boundary fixed points have the same locally dynamical property on Σ after a permutation of the indices $\{1, 2, 3\}$. Then we classify all 3D Ricker maps (10) admitting a carrying simplex by this equivalence, and derive a total of 33 stable equivalence classes. Thus we can investigate the qualitative properties of the orbits, bifurcations and the occurrence of heteroclinic cycles within each class. Classes $1-18$ have trivial dynamics, i.e. all nontrivial orbits converge to fixed points on $\partial\Sigma$. It is shown that Neimark-Sacker bifurcations do not occur in classes $19-25$ and class 32 while they do occur in classes $26-31$. Therefore, there exist some maps from classes $26-31$ possessing closed invariant curves on Σ. Numerical experiments show that the Ricker model can possess attracting quasiperiodic curves on the carrying simplex. Class 29 can also admit Chenciner bifurcations, which imply that two isolated closed invariant curves can coexist on the carrying simplex in this class. Each map from class 27 always has a heteroclinic cycle, i.e. a cyclic arrangement of saddle fixed points and heteroclinic connections. The stability criteria on heteroclinic cycles are provided further. Cushing [9], Davydova *et al.* [10] and Jiang *et al.* [34] also found this cyclical fluctuation phenomenon in many other models. When both the positive fixed point and the heteroclinic cycle are repelling for the map in class 27, numerical simulations show that there may also exist an attracting invariant closed curve on the carrying simplex surrounding the positive fixed point.

Unlike the Atkinson–Allen models and Leslie–Gower models, which always admit a carrying simplex [33], the carrying simplex will break when the growth rates ν_i are large for Ricker models. By specific examples we numerically show that the carrying simplex disappears while chaotic attractors occur as the growth rates increase. We also construct a 4D Ricker map to admit a carrying simplex containing a chaotic attractor, which is first found for competitive mappings. This also implies that for 4D or higher dimensional Ricker maps, chaotic attractors can occur in the carrying simplex. Moreover, in this example, two routes to chaos are detected; one is quasiperiod-doubling cascades leading to chaos, and the other is cascades of homoclinic-doubling bifurcations leading to chaos. These phenomena are also first found for competitive mappings which admit a carrying simplex.

The paper is organized as follows. Section 2 are some notations. In Section 3, we recall the results on the existence of carrying simplex and the index formula.

We provide conditions to guarantee that the Ricker map (10) admits a carrying simplex, and prove that any 2D map admitting a carrying simplex has trivial dynamics. In Section 4, we define an equivalence relation on the space of all 3D Ricker maps admitting a carrying simplex and derive a total of 33 stable equivalence classes. The dynamics within each class is studied further. In section (5), we study the routes to chaos and the relation between chaos and the carrying simplex numerically. In the appendix, the 33 stable equivalence classes in terms of simple inequalities on the parameters are listed in Table A.1. We also present the corresponding phase portraits on their carrying simplices.

2. Notation

Throughout this paper, we reserve the symbol n for the dimension of the euclidean space $\mathbb{R}^n$ and the symbol N for the set $\{1, \cdots, n\}$. We will denote by $\{e_{\{1\}}, \cdots, e_{\{n\}}\}$ the usual basis for $\mathbb{R}^n$. The usual nonnegative cone will be denoted by $\mathbb{R}^n_+ := \{x \in \mathbb{R}^n : x_i \geq 0, \forall i \in N\}$. The interior of $\mathbb{R}^n_+$ is the open cone $\dot{\mathbb{R}}^n_+ := \{x \in \mathbb{R}^n_+ : x_i > 0, \forall i \in N\}$ and the boundary of $\mathbb{R}^n_+$ is $\partial\mathbb{R}^n_+ := \mathbb{R}^n_+ \setminus \dot{\mathbb{R}}^n_+$. We write $\mathbb{Z}_+$ for the set of nonnegative integers. Let $\mathbb{H}_J = \{x \in \mathbb{R}^n : x_j = 0 \text{ for } j \notin J\}$, $\mathbb{H}^+_J = \mathbb{H}_J \cap \mathbb{R}^n_+$, and $\dot{\mathbb{H}}^+_J = \{x \in \mathbb{H}^+_J : x_j > 0 \text{ for } j \in J\}$, where $\emptyset \neq J \subseteq N$. We denote by $\mathbb{H}^+_{\{i\}}$ the ith positive coordinate axis and by $\pi_i = \{x \in \mathbb{R}^n_+ : x_i = 0\}$ the ith coordinate plane. The symbol 0 stands for both the origin of $\mathbb{R}^n$ and the real number 0.

Given two points x, z in $\mathbb{R}^n$, we write $x \leq z$ if $z - x \in \mathbb{R}^n_+$, $x < z$ if $z - x \in \mathbb{R}^n_+ \setminus \{0\}$, and $x \ll z$ if $z - x \in \dot{\mathbb{R}}^n_+$. The reverse relations are denoted by $\geq, >, \gg$, respectively.

Let $X \subset \mathbb{R}^n$. For a map $T : X \to X$, we denote the positive orbit (trajectory) emanating from $y \in X$ for T by the set $\{y(j) : j \in \mathbb{Z}_+\}$, where $y(j) = T^j(y)$ with $y(0) = y$. A set $V \subset X$ is positively invariant under T, if $T(V) \subset V$ and invariant if $T(V) = V$. A fixed point y of T is a point $y \in X$ such that $T(y) = y$. We call $z \in X$ a k-periodic point of T if there exists some positive integer $k > 1$, such that $T^k(z) = z$ and $T^m(z) \neq z$ for any positive integer $m < k$. The k-periodic orbit of the k-periodic point z, $\{z, z(1), z(2), \ldots, z(k-1)\}$, is often called periodic orbit for short. A quasiperiodic curve is a simple closed invariant curve with every orbit being dense.

Given a $k \times k$ square matrix A, we write $A \geq 0$ if A is a nonnegative matrix (i.e., all its entries are nonnegative) and $A > 0$ if A is a positive matrix (i.e., all its entries are positive). The spectral radius of A, denoted by $\rho(A)$, is defined to be the maximum of the norms of its eigenvalues. Given $\emptyset \neq J \subseteq N$, we denote by A_J the submatrix of A with rows and columns from J. We shall ambiguously use I to denote the identity matrix and the identity mapping.

A map $T : \mathbb{R}^n_+ \to \mathbb{R}^n_+$ is competitive (or retrotone) in a subset $W \subset \mathbb{R}^n_+$ if for all $x, z \in W$ with $Tx < Tz$ one has that $x_i < z_i$ provided $z_i > 0$.

A *carrying simplex* for the map T is a subset Σ of $\mathbb{R}^n_+ \setminus \{0\}$ with the following properties:

(P1) Σ is compact, invariant and unordered;

(P2) Σ is homeomorphic via radial projection to the $(n-1)$-dimensional standard probability simplex $\Delta^{n-1} = \{x \in \mathbb{R}^n_+ : \sum_i x_i = 1\}$;

(P3) for any $x \in \mathbb{R}^n_+ \setminus \{0\}$, there exists some $z \in \Sigma$ such that $\lim_{j\to\infty} |T^j(x) - T^j(z)| = 0$;

(P4) $T(\Sigma) = \Sigma$, and $T : \Sigma \mapsto \Sigma$ is a homeomorphism.

We denote the boundary of the carrying simplex Σ relative to $\mathbb{R}^n_+$ by $\partial\Sigma = \Sigma \cap \partial\mathbb{R}^n_+$ and the interior of Σ relative to $\mathbb{R}^n_+$ by $\dot{\Sigma} = \Sigma \setminus \partial\Sigma$.

Assume that

$$\nu_i < \mu_{ii} / \sum_{j=1}^{n} \mu_{ij},\ i = 1, \cdots, n, \text{ or } \nu_i < 1/(\sum_{j=1}^{n} \frac{\mu_{ij}}{\mu_{jj}}),\ i = 1, \cdots, n. \tag{12}$$

We denote the set of all maps taking $\mathbb{R}^n_+$ into itself by $\mathcal{T}(\mathbb{R}^n_+)$ and the set of all Ricker maps on $\mathbb{R}^n_+$ which satisfy (12) by $\mathrm{CRC}(n)$. In symbols:

$$\mathrm{CRC}(n) := \{T \in \mathcal{T}(\mathbb{R}^n_+) : T_i(x) = x_i \exp(\nu_i(1 - \sum_{j=1}^{n} \mu_{ij} x_j)), \nu_i, \mu_{ij} > 0, (12) \text{ holds}, i, j \in N\}.$$

Let U be the $n \times n$ matrix with entries μ_{ij}, and $\mathcal{E}(T)$ be the set of the fixed points of $T \in \mathrm{CRC}(n)$, i.e. $\mathcal{E}(T) = \{x \in \mathbb{R}^n_+ : T(x) = x\}$.

Definition 2.1. *Let $T, \hat{T} \in \mathrm{CRC}(n)$. T and $\hat{T}$ are said to be equivalent relative to $\partial\Sigma$ if there exists a permutation σ of N, such that T has a nontrivial fixed point $q_J \in \mathcal{E}(T) \cap \dot{\mathbb{H}}^+_J$ if and only if $\hat{T}$ has a nontrivial fixed point $\hat{q}_{\sigma(J)} \in \mathcal{E}(\hat{T}) \cap \dot{\mathbb{H}}^+_{\sigma(J)}$, and further q_J has the the same hyperbolicity and local dynamics as $\hat{q}_{\sigma(J)}$ for any $\emptyset \neq J \subsetneqq N$.*

Definition 2.2. *A map $T \in \mathrm{CRC}(n)$ is said to be stable relative to $\partial\Sigma$ if all the fixed points on $\partial\Sigma$ are hyperbolic. We say that an equivalence class is stable if each mapping in it is stable relative to $\partial\Sigma$.*

3. Preliminaries

From now on we assume that $T(x) = (x_1 G_1(x), \cdots, x_n G_n(x)) : \mathbb{R}^n_+ \to \mathbb{R}^n_+$ is a C^1 map with $G_i(x) > 0$ for all $x \in \mathbb{R}^n_+$. Note that this implies that $T_i(x) > 0$ if and only if $x_i > 0$ and, in particular, that $T^{-1}(\{0\}) = \{0\}$.

3.1. The existence of carrying simplex

For the map T, Hirsch developed a theory on the existence of a carrying simplex in [25], where the conclusions were only stated, but not proved. By applying his result to the Ricker map, he proved that the Ricker map (10) admits a carrying simplex if the parameters satisfy (12). The statement of Hirsch's Theorem in [25] was rigorously proved by Ruiz-Herrera [49] under similar assumptions to Hirsch's. However, here we use the readily checked criterion provided by Jiang and Niu [33] to check that the Ricker map (10) admits a carrying simplex under the condition (12), which is easier to verify in application. So we first recall the criterion provided in [33] on the existence of a carrying simplex for the map T.

Theorem 3.1 (Existence Criterion of Carrying Simplex [33])**.** *Suppose that*

$\Upsilon1)$ $\partial G_i(x)/\partial x_j < 0$ *holds for any* $x \in \mathbb{R}^n_+$ *and* $i, j \in N$;

$\Upsilon2)$ $\forall i \in N$, $T|_{\mathbb{H}^+_{\{i\}}} : \mathbb{H}^+_{\{i\}} \to \mathbb{H}^+_{\{i\}}$ *has a fixed point* $q_{\{i\}} = q_i e_{\{i\}}$ *with* $q_i > 0$;

$\Upsilon3)$ $\forall x \in [0, q] \setminus \{0\}$, $G_i(x) + \sum_{j\in\kappa(x)} x_j \frac{\partial G_i(x)}{\partial x_j} > 0$ *holds for any* $i \in \kappa(x)$ (*or* $G_i(x) + \sum_{j\in\kappa(x)} x_i \frac{\partial G_i(x)}{\partial x_j} > 0$ *holds for any* $i \in \kappa(x)$), *where* $\kappa(x) = \{j : x_j > 0\}$ *is the support of* x *and* $q = \sum q_{\{i\}} = (q_1, \cdots, q_n)$.

Then T *possesses a carrying simplex* Σ.

Condition $\Upsilon1)$ means that $G_i(y) < G_i(x)$ for all $i \in N$ provided $x < y$. This follows from

$$G_i(y) - G_i(x) = \int_0^1 DG_i(x_s)(y - x)ds,$$

where $x_s = x + s(y - x)$ with $s \in [0, 1]$. Together with $\Upsilon2)$, $\Upsilon1)$ implies $G_i(0) > G_i(q_{\{i\}}) = 1$ for all $i \in N$, so 0 is a hyperbolic repeller for T. $\Upsilon3)$ implies that $\det DT(x) > 0$ for all $x \in [0, q]$, and together with $\Upsilon1)$ it guarantees $(DT(x)_{\kappa(x)})^{-1} > 0$ for all $x \in [0, q] \setminus \{0\}$ by the proof of Theorem 3.1 in [33]. Therefore, T is competitive and one-to-one in $[0, q]$ by Proposition 4.1 in [49].

It is easy to check that the Ricker map (10) satisfies $\Upsilon3)$ in Theorem 3.1 if condition (12) holds, so each map $T \in \mathrm{CRC}(n)$ satisfies the conditions $\Upsilon1)$–$\Upsilon3)$ in Theorem 3.1. Therefore, every Ricker map in CRC(n) is competitive in $[0, q]$, and moreover, we have the following.

Proposition 3.1. *Every map* $T \in \mathrm{CRC}(n)$ *admits a carrying simplex* Σ.

Theorem 3.2. *Consider the two-dimensional map* $T(x_1, x_2) = (x_1G_1(x), x_2G_2(x))$ *taking* $\mathbb{R}^2_+$ *into* $\mathbb{R}^2_+$. *If* T *admits a carrying simplex* Σ, *then it has trivial dynamics, i.e. every nontrivial orbit converges to some fixed point on* Σ.

Proof. Note that $T(\Sigma) = \Sigma$. Consider the homeomorphism $T|_\Sigma : \Sigma \to \Sigma$, where $T|_\Sigma$ is the restriction of T on Σ. Since Σ is homeomorphic to $\Delta^1 = \{x \in \mathbb{R}^2_+ : x_1 + x_2 = 1\}$, there exists a homeomorphism h taking $[0,1]$ onto Σ. Thus,

$$f = h^{-1} \circ T|_\Sigma \circ h : [0,1] \to [0,1]$$

is a homeomorphism which is topologically conjugate to $T|_\Sigma$ and $0, 1$ are its two fixed points. It follows that f is a strictly increasing function. Take $x \in [0,1]$. If x is not fixed, i.e. $f(x) \neq x$, then without loss of generality, assume that $x < f(x)$. So, we obtain that

$$0 < x < f(x) < \cdots < f^{k-1}(x) < f^k(x) < \cdots < 1.$$

Therefore, there exists some fixed point $\alpha \in [0,1]$ such that $f^k(x) \to \alpha$ as $k \to \infty$. At this moment, we have proved that each orbit of $T|_\Sigma$ converges to some fixed point on Σ. Then together with the property (P3) of Σ, one can obtain the result. $\square$

Corollary 3.1. *Any two-dimensional map* (1) *satisfying the conditions* $\Upsilon 1)-\Upsilon 3)$ *in Theorem 3.1 has trivial dynamics. In particular, every map* $T \in \mathrm{CRC}(2)$ *has trivial dynamics.*

Remark 3.1. *Since the carrying simplex is codimension-one, a 1D map admitting a carrying simplex is equivalent to the fact that it possesses a positive fixed point attracting all nontrivial points. Theorem 3.2 and Corollary 3.1 imply that such 2D maps also have trivial dynamics, in which chaos even periodic motions cannot appear. Such trivial dynamics for 2D discrete-time competitive systems defined on* $[0, q]$ *was also analyzed by an alternative way in [53].*

Roughly speaking, Proposition 3.1 states that the Ricker map (10) *admits a carrying simplex when the growth rates* $\nu_i > 0$ *are small. Indeed, when some* ν_i *is sufficiently big, even the dynamics of species* i *in the absence of the others becomes chaotic, and hence the carrying simplex will break, because* $\partial\Sigma$ *contains any carrying simplex of each subsystem restricted to the boundary and the carrying simplex* $\partial\Sigma \cap \mathbb{H}^+_{\{i\}}$ *is a fixed point for the 1D map* $T|_{\mathbb{H}^+_{\{i\}}}$ *which implies that every orbit on* $\mathbb{H}^+_{\{i\}}$ *cannot be chaotic. In section 5, we numerically show that the carrying simplex breaks while chaos occurs as the growth rates increase by specific examples in detail. Moreover, for 4D or higher dimensional systems, strange attractors do occur in the carrying simplex, i.e. the carrying simplex may contain some strange attractors.*

3.2. The index formula on the carrying simplex

Let $F = T - I$. Let x be a fixed point of T, that is, a zero of F. The index of T at x is denoted by $\mathscr{I}(x, T)$ and the degree of F at x is denoted by $\mathscr{V}(x, F)$.

If $\det DF(x) \neq 0$, we have

$$\mathscr{I}(x,T) = \mathscr{V}(x,-F) = (-1)^n \mathrm{sgn}(\det DF(x)) = (-1)^n \mathscr{V}(x,F).$$

Assume $n=3$. We call the fixed point x of the map $T : \mathbb{R}^3_+ \to \mathbb{R}^3_+$ an *axial* fixed point if it is on some coordinate axis; a *planar* fixed point if it lies in the interior of some coordinate plane; and a *positive* fixed point if it is in $\dot{\mathbb{R}}^3_+$. Denote the set of all nontrivial axial, planar, and positive fixed points by $\mathcal{E}_v$, $\mathcal{E}_s$, and $\mathcal{E}_p$, respectively. For the reader's convenience, we recall the index formula in [32].

Lemma 3.1 (Theorem 3.2 in [32])**.** *Suppose that $T : \mathbb{R}^3_+ \to \mathbb{R}^3_+$ is given by* (1) *and satisfies $\partial G_i/\partial x_j < 0$ for any $x \in \mathbb{R}^3_+$. Assume further that T possesses a carrying simplex Σ and the continuous-time system $\dot{x} = F(x) = T(x) - x$ is dissipative with the origin 0 being a repeller. If T has only finitely many fixed points on Σ and 1 is not an eigenvalue of any of their Jacobian matrices, then*

$$\sum_{\theta \in \mathcal{E}_v} \mathscr{I}(\theta,T) + 2\sum_{\theta \in \mathcal{E}_s} \mathscr{I}(\theta,T) + 4\sum_{\theta \in \mathcal{E}_p} \mathscr{I}(\theta,T) = 1.$$

Now we consider the map $T \in \mathrm{CRC}(3)$. Suppose that all fixed points of T are isolated. Besides the trivial fixed point 0, T has three axial fixed points $q_{\{1\}} = (1/\mu_{11}, 0, 0)$, $q_{\{2\}} = (0, 1/\mu_{22}, 0)$, $q_{\{3\}} = (0, 0, 1/\mu_{33})$. In the interior of π_i, there may exist a planar fixed point $v_{\{i\}}$ satisfying

$$\mu_{ji}x_i + \mu_{jj}x_j + \mu_{jk}x_k = 1,\ x_i = 0,\ i \neq j \neq k \neq i. \tag{13}$$

T may also admit a positive fixed point p in $\dot{\mathbb{R}}^3_+$ which satisfies

$$\mu_{i1}x_1 + \mu_{i2}x_2 + \mu_{i3}x_3 = 1, \quad i = 1,2,3. \tag{14}$$

Note that the planar fixed point and positive fixed point satisfy linear equations (13) and (14), respectively, so the planar fixed point in each coordinate plane or the positive fixed point is unique if they exist. We set $\mathscr{I}(v_{\{i\}},T) = 0$ ($\mathscr{I}(p,T) = 0$), if the planar (positive) fixed point $v_{\{i\}}$ (p) does not exist. The following corollary follows from the above analysis and Lemma 3.1 immediately.

Corollary 3.2. *Consider $T \in \mathrm{CRC}(3)$. If the fixed points are isolated and 1 is not an eigenvalue of each of Jacobian matrices at the fixed points on Σ, then we have*

$$\sum_{i=1}^{3}(\mathscr{I}(q_{\{i\}},T) + 2\mathscr{I}(v_{\{i\}},T)) + 4\mathscr{I}(p,T) = 1.$$

Remark 3.2. *Let $T \in \mathrm{CRC}(n)$. If T admits a unique positive fixed point $p = (p_1, \cdots, p_n)$, i.e.,*

$$(Ux^\tau)_i = 1, \quad i = 1, \cdots, n \tag{15}$$

has a unique positive solution, then 1 is not an eigenvalue of $DT(p) = I - \mathrm{diag}[p_i\nu_i]U$, where $\mathrm{diag}[p_i\nu_i]$ denotes the diagonal matrix with the diagonal entries $p_i\nu_i$. Otherwise, 0 is an eigenvalue of the matrix $\mathrm{diag}[p_i\nu_i]U$, and hence $\det U = 0$. Then (15) has either no solution, or infinitely many solutions, a contradiction. Therefore, the index of p is either 1 or -1. Note that $(Up^\tau)_i = 1$, so the sum of the ith row of the positive matrix $M := \mathrm{diag}[\nu_i]U\mathrm{diag}[p_i]$ is $\nu_i < 1$ (see (12)). It then follows from Perron-Frobenius theorem that $0 < \rho(M) < 1$ is an eigenvalue of M and the magnitudes of the other eigenvalues are all less than 1. Set $\lambda^* := 1 - \rho(M)$. Since $\mathrm{diag}[p_i\nu_i]U$ and M have the same eigenvalues, $0 < \lambda^* < 1$ is a real eigenvalue of $DT(p)$ whose associated eigenvector is strictly positive and all the other eigenvalues possess real parts greater than 0 and less than 2.

4. Dynamics of Ricker maps

In this section, we analyze the dynamics of the map $T \in \mathrm{CRC}(3)$:

$$T_i(x) = x_i(\exp(\nu_i(1 - \mu_{i1}x_1 - \mu_{i2}x_2 - \mu_{i3}x_3))), \ i = 1, 2, 3. \tag{16}$$

Recall that each $T \in \mathrm{CRC}(3)$ admits a 2-dimensional carrying simplex Σ which is homeomorphic to Δ^2. Each coordinate plane π_i is invariant under T, and the restriction of T to it is a 2-dimensional map $T|_{\pi_i} \in \mathrm{CRC}(2)$, which admits a one-dimensional carrying simplex, so $\partial\Sigma$ is composed of the one-dimensional carrying simplices of the restricted maps $T|_{\pi_i}$.

4.1. Classification of the 2-dimensional maps

In this subsection, we study the map $T \in \mathrm{CRC}(2)$:

$$T_i(x) = x_i(\exp(\nu_i(1 - \mu_{i1}x_1 - \mu_{i2}x_2))), \ i = 1, 2, \tag{17}$$

which takes $\mathbb{R}^2_+$ into itself. T admits a one-dimensional carrying simplex Σ which is homeomorphic to Δ^1, and Corollary 3.1 implies that any map $T \in \mathrm{CRC}(2)$ has trivial dynamics. A detailed analysis of the dynamics is given below.

Besides the trivial fixed point 0 which is a hyperbolic repeller, T admits two axial fixed points $q_{\{1\}} : (1/\mu_{11}, 0)$, $q_{\{2\}} : (0, 1/\mu_{22})$. The fixed point $q_{\{i\}}$ is just the intersection of the line $S_i = \{x \in \mathbb{R}^2_+ : \mu_{ii}x_i + \mu_{ij}x_j = 1, i \neq j\}$ and the x_i-coordinate axis. If S_1 and S_2 intersect in $\dot{\mathbb{R}}^2_+$, then there also exists a positive fixed point p at the intersection of S_1 and S_2.

The *basic reproduction ratio of species j in an environment set by species i* is

$$R_{ij} = R_0^{(j)} e^{-\nu_j \mu_{ji} q_{\{i\}}} = e^{\nu_j \left(1 - \frac{\mu_{ji}}{\mu_{ii}}\right)} \tag{18}$$

Clearly, $R_{ij} > 1$ ($R_{ij} < 1$) if and only if $\gamma_{ij} := \mu_{ii} - \mu_{ji} > 0$ ($\gamma_{ij} < 0$).

Set $\mathbb{R}^2_+ \setminus S_i = U_i \cup B_i$, where U_i and B_i are the unbounded and bounded disjoint components of $\mathbb{R}^2_+ \setminus S_i$, respectively. Then $q_{\{i\}} \in U_j$ (B_j) if and only if $R_{ij} < 1$ (> 1).

The following is an immediate result by Corollary 3.1; see also [53] for a similar analysis.

Lemma 4.1. *Let $T \in \mathrm{CRC}(2)$.*

(a) *If $R_{12} < 1, R_{21} > 1$, then the positive fixed point p does not exist and $q_{\{1\}}$ attracts all points not on the x_2-axis.*
(b) *If $R_{12} > 1, R_{21} < 1$, then the positive fixed point p does not exist and $q_{\{2\}}$ attracts all points not on the x_1-axis.*
(c) *If $R_{12}, R_{21} > 1$, then T has a hyperbolic positive fixed point p attracting all points in $\dot{\mathbb{R}}^2_+$.*
(d) *If $R_{12}, R_{21} < 1$, then T has a positive fixed point p which is a hyperbolic saddle. Moreover, every nontrivial orbit tends to one of the asymptotically stable nodes $q_{\{1\}}$ or $q_{\{2\}}$ or to the saddle p.*

Remark 4.1. *The statements of Lemma 4.1 have clear biological interpretations, which we present here.*

(i) If $R_{ij} > 1$, then species j can invade species i while it cannot invade if $R_{ij} < 1$.
(ii) If species j can invade species i but not vice versa, then species i is driven to extinction, whilst species j remains extant.
(iii) In the case of mutual invadabilty, that is, if both species can invade the other, then there will be coexistence in the form of an asymptotically stable positive fixed point.
(iv) If neither species can invade (mutual noninvadability), there is no coexistence: One of the species will oust the other. The surviving species depends on the initial conditions. (Convergence to the positive saddle happens only for initial conditions in a set of measure zero and is hence impossible in nature).

The situations mentioned above are of particular interest when the two populations 1 and 2 are not different species, but different traits (resident and mutant) of the same species. To begin with, the resident ($i = 1$) is at the fixed point $q_{\{1\}}$ and then the mutant $q_{\{2\}}$ is introduced in small quantities. Case (i) $R_{12} > 1$

gives the condition for successful invasion. Case (ii) describes trait substitution. Case (iii) is an example of protected dimorphism. For a discussion of these notions and their consequences for evolutionary dynamics we refer the reader to [14, 15, 16, 17].

Corollary 4.1. *There are a total of* 3 *stable equivalence classes in* CRC(2)*. The three dynamical scenarios are presented in Fig.* 1*.*

Figure 1: The dynamics in Σ replaced by Δ^1. A closed dot $\bullet$ stands for a fixed point which attracts on Σ, and an open dot $\circ$ stands for the one which repels on Σ. Each Σ denotes an equivalence class. The first class corresponds to case (a) or (b) in Lemma 4.1; the second class corresponds to case (c) in Lemma 4.1; the third class corresponds to case (d) in Lemma 4.1.

Remark 4.2. *Suppose that* $T \in \mathrm{CRC}(2)$ *is stable relative to* $\partial\Sigma$ *and possesses a positive fixed point* p*. Then* $\det U \neq 0$*, and the positive fixed point* p *is unique. Moreover,* p *attracts on* Σ *if and only if* $\det U > 0$ (Lemma 4.1(c)) *and repels on* Σ *if and only if* $\det U < 0$ (Lemma 4.1(d))*.*

Biologically, $\det U > 0$ *means that both species can invade, while* $\det U < 0$ *means that none of them can* (Remark 4.1(i))*.*

For other related results on the dynamics of the 2D Ricker map (17), see, for example, [1, 6, 7, 31, 40, 50, 51].

4.2. Classification of the 3-dimensional maps

Now we analyze the 3-dimensional map (16). Hereafter, denote by S_i the plane $\{x \in \mathbb{R}^3_+ : \mu_{ii}x_i + \mu_{ij}x_j + \mu_{ik}x_k = 1, i, j, k \text{ are distinct}\}$. Let $\mathbb{R}^3_+ \setminus S_i = U_i \cup B_i$, where U_i and B_i are the unbounded and bounded disjoint components of $\mathbb{R}^3_+ \setminus S_i$, respectively.

Note that the trivial fixed point 0 is a hyperbolic repeller since the eigenvalues of $DT(0)$ are $R_0^{(i)} = e^{\nu_i} > 1$, $i = 1, 2, 3$. Recall that $q_{\{1\}} = (1/\mu_{11}, 0, 0)$, $q_{\{2\}} = (0, 1/\mu_{22}, 0)$, $q_{\{3\}} = (0, 0, 1/\mu_{33})$ are three axial fixed points of T. If S_i, S_j and π_k intersect in $\mathbb{R}^3_+$, then T has a fixed point $v_{\{k\}}$. T admits a positive fixed point p if and only if S_i, S_j and S_k intersect in $\dot{\mathbb{R}}^3_+$. Let

$$\gamma_{ij} := \mu_{ii} - \mu_{ji}, \quad \beta_{ij} = \frac{\mu_{jj} - \mu_{ij}}{\mu_{ii}\mu_{jj} - \mu_{ij}\mu_{ji}} \tag{19}$$

for $i, j = 1, 2, 3$ and $i \neq j$.

By the invariance of π_i and the analysis of the 2-dimensional case in §4.1, the classification program, statements, proofs in [32] carry over to CRC(3) in a straightforward way, so we do not re-do it unless the need for special details.

Lemma 4.2. *If $\gamma_{ij} > 0$ (< 0) then $q_{\{i\}}$ repels (attracts) along $\partial\Sigma \cap \pi_k$, where i, j, k are distinct. Furthermore, if $\gamma_{ij}, \gamma_{ik} > 0$ (< 0) then the fixed point $q_{\{i\}}$ is a repeller (an attractor) on Σ; if $\gamma_{ij}\gamma_{ik} < 0$, then the fixed point $q_{\{i\}}$ is a saddle on Σ; and $q_{\{i\}}$ is hyperbolic if and only if $\gamma_{ij}\gamma_{ik} \neq 0$.*

Lemma 4.3. *If $\gamma_{jk}\gamma_{kj} > 0$ then T admits a fixed point $v_{\{i\}}$ in the interior of the coordinate plane π_i, where i, j, k are distinct. Moreover, if $\gamma_{jk}, \gamma_{kj} < 0$ (> 0) then $v_{\{i\}}$ repels (attracts) along $\partial\Sigma$.*

Lemma 4.4. *Suppose that the planar fixed point $v_{\{i\}}$ exists. Then $(Uv^{\tau}_{\{i\}})_i < 1$ (> 1) implies that $v_{\{i\}}$ locally repels (attracts) in $\dot{\Sigma}$. Moreover, $v_{\{i\}}$ is hyperbolic if and only if $(Uv^{\tau}_{\{i\}})_i \neq 1$.*

Remark 4.3. *It is easy to check that*

$$(Uv^{\tau}_{\{k\}})_k < 1 \ (> 1) \Leftrightarrow \mu_{ki}\beta_{ij} + \mu_{kj}\beta_{ji} < 1 \ (> 1) \Leftrightarrow v_{\{k\}} \in B_k \ (U_k).$$

A map $T \in \mathrm{CRC}(3)$ is stable relative to $\partial\Sigma$ if and only if $\gamma_{ij} \neq 0$ and $\mu_{ki}\beta_{ij} + \mu_{kj}\beta_{ji} \neq 1$, i.e., $(Uv^{\tau}_{\{k\}})_k \neq 1$ (if $v_{\{k\}}$ exists). Suppose that T is stable relative to $\partial\Sigma$. If T admits a positive fixed point p which satisfies (14), then p is the unique positive fixed point. Otherwise, assume that T has two different positive fixed points p and $\tilde{p}$. Now $p_s := sp + (1-s)\tilde{p}$ is a solution of (14) for any $s \geq 0$. Let $\bar{s} := \sup\{s > 0 : p_s \in \Sigma\}$. Then $p_{\bar{s}} \in \partial\Sigma$ is a fixed point, which is not hyperbolic, contradicting that T is stable relative to $\partial\Sigma$.

Proposition 4.1. *Suppose that $T \in \mathrm{CRC}(3)$ is stable relative to $\partial\Sigma$. Then we have the formula*

$$\sum_{i=1}^{3}(\mathscr{I}(q_{\{i\}}, T) + 2\mathscr{I}(v_{\{i\}}, T)) + 4\mathscr{I}(p, T) = 1. \tag{20}$$

Proposition 4.2. *Assume that $T \in \mathrm{CRC}(3)$ is stable relative to $\partial\Sigma$. Then $\mathscr{I}(q_{\{i\}}, T) = 1$ $(\mathscr{I}(v_{\{i\}}, T) = 1)$ if $q_{\{i\}}$ $(v_{\{i\}})$ is a repeller or an attractor on Σ and $\mathscr{I}(q_{\{i\}}, T) = -1$ $(\mathscr{I}(v_{\{i\}}, T) = -1)$ if $q_{\{i\}}$ $(v_{\{i\}})$ is a saddle on Σ. Moreover, the positive fixed point p exists if and only if $\mathscr{I}(p, T) \neq 0$.*

Remark 4.4. *For a map $T \in \mathrm{CRC}(3)$ which is stable relative to $\partial\Sigma$, Propositions 4.1-4.2 imply that the existence of the positive fixed point p and its index can be determined by the local dynamics of boundary fixed points. By Remark 3.2, the index of p is either 1 or -1 or 0 (if it does not exist). Moreover, $\mathscr{I}(q_{\{i\}}, T) = \mathrm{sgn}(\gamma_{ij}\gamma_{ik})$; if $v_{\{k\}}$ exists, i.e. $\gamma_{ij}\gamma_{ji} > 0$, then $\mathscr{I}(v_{\{k\}}, T) = \mathrm{sgn}(\gamma_{ij}(\mu_{ki}\beta_{ij} + \mu_{kj}\beta_{ji} - 1))$.*

Theorem 4.1. *There are a total of 33 stable equivalence classes in $\mathrm{CRC}(3)$.*

It is a straightforward combinatorial task on the non-zero values of $\mathrm{sgn}(\gamma_{ij})$ and $\mathrm{sgn}(\mu_{ki}\beta_{ij}+\mu_{kj}\beta_{ji}-1)$ (if $v_{\{k\}}$ exists) to classify the stable equivalence classes by Remark 4.3, which is based on the index formula (20) and a geometric analysis of the positions of the planes S_j. We list the 33 stable equivalence classes in Table A.1, which can be obtained by the following three steps. Given $\mu_{ij}, \nu_i > 0$ such that (12) holds.

Step 1 The non-zero values of $\mathrm{sgn}(\gamma_{ij})$ constitute 2^6 possibilities which reduce to 16 possibilities modulo permutation of the indices.

Step 2 Under the given values of $\mathrm{sgn}(\gamma_{ij})$ one can determine the existence or nonexistence of the fixed points $v_{\{k\}}$. Then applying formula (20) to each of the 16 possibilities obtained in Step 1, we count 57 possibilities for the indices of all the fixed points on the corresponding Σ, which reduce to 45 possibilities modulo permutation of the indices. According to Remark 4.4, the index of $v_{\{k\}}$ determines the non-zero value of $\mathrm{sgn}(\mu_{ki}\beta_{ij}+\mu_{kj}\beta_{ji}-1)$, and hence the position of $v_{\{k\}}$ relative to S_k.

Step 3 By the position of $q_{\{i\}}$ relative to S_j $(i \neq j)$ and the position of $v_{\{k\}}$ relative to S_k, which are all inequalities on μ_{ij}, one can rule out 12 nonexistent cases. Then we derive the total of 33 stable equivalence classes and together with condition (12) we obtain the parameter conditions for each class.

The phase portrait on the carrying simplex for each of the 33 stable equivalence classes in CRC(3) is presented in Table A.1. The corresponding parameter conditions of a representative element with a concrete example for each class are also given. Any map in CRC(3) which is stable relative to $\partial\Sigma$ belongs to one of the classes in Table A.1 (modulo permutation of the indices). The maps in classes $1-18$ have no positive fixed point because $\mathscr{I}(p,T)=0$ by the indices of boundary fixed points and formula (20). We show in §4.3 that all these classes have trivial dynamics, i.e. every orbit of each map in these classes tends to some fixed point on $\partial\Sigma$, and present the whole dynamics on Σ further. Nontrivial dynamics (e.g. Neimark-Sacker bifurcations) can only occur in the other 15 classes which all have a unique positive fixed point p, where $\mathscr{I}(p,T)=-1$ for classes $19-25$, and $\mathscr{I}(p,T)=1$ for classes $26-33$.

Remark 4.5. *Given $\mu_{ij}, \bar{\nu_i} > 0$ satisfying* (12)*, μ_{ij}, ν_i also satisfy* (12) *for any $0 < \nu_i \leq \bar{\nu_i}$, so the map* (16) *with the parameters μ_{ij}, ν_i is still in* CRC(3) *and belongs to the same stable class as the one with the parameters $\mu_{ij}, \bar{\nu_i}$.*

4.3. Dynamics on the carrying simplex

In this subsection, we consider the detailed dynamics on the carrying simplex for each stable equivalence class in CRC(3). Since each map from any of classes

1 to 18 in Table A.1 does not have a positive fixed point, together with Ruiz-Herrera's exclusion criterion [49, Theorem 2.2], we obtain the following trivial dynamics immediately.

Theorem 4.2. *Each map from any of classes* $1-18$ *has trivial dynamics, i.e. every nontrivial orbit converges to some fixed point on* $\partial\Sigma$.

Now we focus on the classes 19 to 33. Note that each map in them has a unique positive fixed point $p=(p_1,p_2,p_3)$ with $DT(p)=I-\mathrm{diag}[p_i\nu_i]U$.

Lemma 4.5. *For each map in classes* $19-25$, *we have* $\mathscr{I}(p,T)=-1$ *and* $\det U<0$; *while for each map in classes* $26-33$, *we have* $\mathscr{I}(p,T)=1$ *and* $\det U>0$.

Proposition 4.3. *The positive fixed point* p *is a repeller on* Σ *in class* 32, *and hence this class cannot admit Neimark-Sacker bifurcations.*

The proofs of Lemma 4.5 and Proposition 4.3 are repetitions of the corresponding proofs of Lemma 4.9 and Proposition 4.5 in [33] just by replacing the matrix $\mathrm{diag}[p_i/c_i]B$ there by $\mathrm{diag}[p_i\nu_i]U$.

Theorem 4.3. *The positive fixed point* p *is a saddle on* Σ *in classes* $19-25$, *and every nontrivial orbit converges to some fixed point on the boundary of the carrying simplex, except those on the stable manifold of* p.

Theorem 4.3 follows from Theorem 3.1 in [44], and moreover, the results in [43] imply that the stable manifold and unstable manifold of the saddle p are simple curves; see Table A.1 for the phase portraits of these classes.

Theorem 4.4. *The positive fixed point* p *is globally asymptotically stable in* $\dot{\mathbb{R}}^3_+$ *for each map in class* 33.

Theorem 4.4 follows from Theorem 2.1 in [20], and the phase portrait on the carrying simplex for class 33 is shown in Table A.1.

Lemma 4.6. *For each Ricker map* T *given by* (16) *having a unique positive fixed point* p *in* $\mathbb{R}^3_+$, *there exists a Ricker map* $\hat{T}$ *given by* (16) *with the unique positive fixed point* $\hat{p}=(1,1,1)$ *topologically equivalent to* T.

Proof. Set $z_i(t)=x_i(t)/p_i$, $i=1,2,3$, where $\{x(t):t\in\mathbb{Z}_+\}$ is the positive trajectory emanating from $x(0)=(x_1,x_2,x_3)$ for T. Thus,

$$\begin{aligned} z_i(t+1) = &\ \tfrac{1}{p_i}x_i(t)\exp(\nu_i(1-\textstyle\sum_{j=1}^3\mu_{ij}x_j(t)))\\ = &\ z_i(t)\exp(\nu_i(1-\textstyle\sum_{j=1}^3\mu_{ij}p_jz_j(t)))\\ = &\ z_i(t)\exp(\nu_i(1-(U\mathrm{diag}[p_j]z(t)^\tau)_i))\\ := &\ z_i(t)\exp(\nu_i(1-(\hat{U}z(t)^\tau)_i)),\end{aligned}$$

where $\hat{U} = U\text{diag}[p_j]$. Hence $\{z(t) : t \in \mathbb{Z}_+\}$ is the positive trajectory emanating from $z(0) = (x_1/p_1, x_2/p_2, x_3/p_3)$ for $\hat{T} = (\hat{T}_1, \hat{T}_2, \hat{T}_3)$ with $\hat{T}_i(z) := z_i \exp(\nu_i(1 - (\hat{U}z^\tau)_i))$, $i = 1, 2, 3$. It follows from $(Up^\tau)_i = 1$ that $(\hat{U}\hat{p}^\tau)_i = 1$, where $\hat{p} = (1, 1, 1)$, i.e., $(1, 1, 1)$ is the unique positive fixed point of $\hat{T}$. It is clear that $\hat{T}$ and T are topologically equivalent. $\square$

By Lemma 4.6, we may assume that the fixed point p of T is at $(1, 1, 1)$ provided it exists. At this moment, the parameters μ_{ij} of T satisfy that $\sum_j \mu_{ij} = 1$, $i = 1, 2, 3$, i.e., the sum of the ith row of $U = (\mu_{ij})_{3\times 3}$ is one. Let $p = (1, 1, 1)$. Then $DT(p) = I - \text{diag}[\nu_i]U$. Hereafter, we always assume that $n = 3$, and $\mu_{ij} > 0$ satisfying $\det U > 0$ and $\sum_j \mu_{ij} = 1$, $i = 1, 2, 3$. Consider the map $T \in \text{CRC}(3)$ with the parameters μ_{ij}, ν_i. Let $A = DT(p) = I - \text{diag}[\nu_i]U$.

Lemma 4.7. *Under the above assumptions, we have*

(a) *If* $\det U_{\{i,j\}} < 0$, *then for* $\nu_k > 0$ *sufficiently small, the matrix* A *has two eigenvalues with magnitudes greater than* 1, *where* i, j, k *are distinct.*

(b) *If* $\det U_{\{i,j\}} > 0$, *then for* $\nu_k > 0$ *sufficiently small, the matrix* A *has two eigenvalues with magnitudes less than* 1, *where* i, j, k *are distinct.*

Proof. Set $M := \text{diag}[\nu_i]U$. Then for definiteness, let $i = 1, j = 2, k = 3$.

(a) By $\det U_{\{1,2\}} < 0$, one has $\det M_{\{1,2\}} < 0$. For $\nu_3 = 0$, the entries in the third row of M are 0, so M has a negative eigenvalue and a positive eigenvalue besides 0. Since the eigenvalues of M depend continuously on the entries of M, and hence on ν_3, thus for $\nu_3 > 0$ sufficiently small, M has an eigenvalue with negative real part. Recall that $\det U > 0$, so $\det M > 0$, which implies that M has two eigenvalues with negative real parts. Therefore, A has two eigenvalues with real parts greater than 1, i.e, A has two eigenvalues with magnitudes greater than 1.

(b) By $\det U_{\{1,2\}} > 0$, one has $\det M_{\{1,2\}} > 0$. So, M has two positive eigenvalues besides 0 for $\nu_3 = 0$ because $M_{\{1,2\}}$ is a positive matrix. It follows from $1 = \mu_{i1} + \mu_{i2} + \mu_{i3}$ that the sum of the ith row of M is ν_i which is less than 1. Then the Perron-Frobenius theorem ensures that both of the two positive eigenvalues are less than 1. Thus A has two eigenvalues with magnitudes less than 1 for $\nu_3 = 0$, and hence for $\nu_3 > 0$ sufficiently small. $\square$

Lemma 4.8. *Under the above assumptions, if* $\det U_{\{i,j\}}$, $i < j$, *are not all of the same sign* (*i.e., at least one is positive and one is negative*), *then for any* $\bar{v}_1, \bar{v}_2, \bar{v}_3 > 0$, *there exist* $0 < \nu_i < \bar{\nu}_i$, $i = 1, 2, 3$, *so that the map* T *with the parameters* μ_{ij}, ν_i *belongs to* CRC(3) *and the matrix* A *possesses a pair of complex conjugate eigenvalues of modulus* 1 *which do not equal* $\pm 1, \pm \mathrm{i}, (-1 \pm \sqrt{3}\mathrm{i})/2$, *where* i *stands for the imaginary unit.*

Proof. Without loss of generality, assume that $\det U_{\{1,2\}} > 0, \det U_{\{1,3\}} < 0$. First choose $0 < \nu_1 = u_1 < \bar{\nu}_1$, $0 < \nu_2 = u_0 < \bar{\nu}_2$, $0 < \nu_3 = v_0 < \bar{\nu}_3$ such that (12) holds. Since $\det U_{\{1,2\}} > 0$, it follows from Lemma 4.7 that there exists $0 < \nu_3 = u_3 < v_0$ sufficiently small such that A has two eigenvalues with magnitudes less than 1. Now fix $\nu_1 = u_1$ and $\nu_3 = u_3$. Since $\det U_{\{1,3\}} < 0$, Lemma 4.7 ensures that A has two eigenvalues with magnitudes greater than 1 for $0 < \nu_2 = \bar{u}_0 < u_0$ sufficiently small. Thus, as ν_2 varies from u_0 to $\bar{u}_0$, at least one of the eigenvalues of A varies continuously from having magnitude less than 1 to magnitude greater than 1, and necessarily crosses the unit circle in the complex plane. Since $\det U \neq 0$, 1 is not an eigenvalue of A. On the other hand, by Remark 3.2 one knows that all the eigenvalues of A have positive real parts. So $-1, \pm\mathrm{i}, (-1 \pm \sqrt{3}\mathrm{i})/2$ are not eigenvalues of A; and moreover, there exists a $0 < u_2 \leq u_0$ such that A has a pair of complex conjugate eigenvalues of modulus 1 as $\nu_2 = u_2$. By Remark 4.5, one can choose $\nu_1 = u_1, \nu_2 = u_2, \nu_3 = u_3$ such that the conclusion holds. □

Given $\mu_{ij} > 0, 0 < \nu_i < 1$ such that $\det U > 0$ and $\sum_{j=1}^{3} \mu_{ij} = 1$, $i, j = 1, 2, 3$. Let $\hat{U} = \mathrm{diag}[\nu_1, 1, \nu_3]U := (\hat{\mu}_{ij})_{3\times 3}$, $\nu_2 = s$, and $M^s = \mathrm{diag}[1, s, 1]\hat{U}$. Denote by $f(z, s) = \det(M^s - zI)$ the characteristic polynomial of M^s. Let $A^s = I - M^s$. Assume that A^s has a pair of complex conjugate eigenvalues of modulus 1 at $0 < s = s_0 < 1$ which do not equal $\pm 1, \pm\mathrm{i}, (-1 \pm \sqrt{3}\mathrm{i})/2$. Now for any s in a small neighborhood V of s_0, A^s has a pair of complex conjugate eigenvalues $w(s), \overline{w(s)}$ with $|w(s_0)| = 1$. We let $w(s) = u(s) + \mathrm{i}v(s)$ for $s \in V$.

Lemma 4.9. *Under the above assumptions,* $\frac{d|w(s)|}{ds}|_{s=s_0} \neq 0$.

Proof. Noticing that
$$\begin{aligned}
&\mathrm{tr}(M^s) = \hat{\mu}_{11} + s\hat{\mu}_{22} + \hat{\mu}_{33},\\
&\det M^s_{\{1,2\}} = s \det \hat{U}_{\{1,2\}},\\
&\det M^s_{\{1,3\}} = \det \hat{U}_{\{1,3\}},\\
&\det M^s_{\{2,3\}} = s \det \hat{U}_{\{2,3\}},\\
&\det M^s = s \det \hat{U},
\end{aligned}$$
the proof is a copy of that of Lemma 4.14 in [33] by replacing $\frac{s}{c_2(s)}$ to be s. □

Theorem 4.5. *Given* $\mu_{ij}, \bar{\nu}_i > 0$ *such that* $\det U > 0$, $\sum_{j=1}^{3} \mu_{ij} = 1$ *and* (12) *holds,* $i, j = 1, 2, 3$. *Consider the map* $T^{[\nu]} \in \mathrm{CRC}(3)$ *given by* (16) *with the parameters* μ_{ij} *and* $0 < \nu_i < \bar{\nu}_i$. *If* $\det U_{\{i,j\}}$, $i < j$, $i, j = 1, 2, 3$, *are not all of the same sign, then there exists some* $\hat{\nu} = (\hat{\nu}_1, \hat{\nu}_2, \hat{\nu}_3)$ *with* $0 < \hat{\nu}_i < \bar{\nu}_i$ *such that the Jacobian matrix* $DT^{[\hat{\nu}]}(p)$ *has a pair of complex conjugate eigenvalues* *of modulus* 1 *which do not equal* $\pm1, \pm\mathrm{i}, (-1 \pm \sqrt{3}\mathrm{i})/2$*, where* $p = (1, 1, 1)$ *is the unique positive fixed point. Furthermore, the restriction of* $T^{[\nu]}$ *to the two dimensional center manifold at the critical parameter value* $\hat{\nu}$ *can be transformed to the complex Poincaré normal form*

$$\omega \mapsto (1+\beta)e^{\mathrm{i}\theta(\beta)}\omega + d(\beta)\omega|\omega|^2 + O(|\omega|^4),\ \omega \in \mathbb{C}, \tag{21}$$

where ω *is a complex variable and* $d(\beta)$ *is a complex function.*

Proof. Let $A^{[\nu]} := DT^{[\nu]}(p) = I - \mathrm{diag}[\nu_i]U$. It follows from Lemma 4.8 that there exist $0 < \hat{\nu}_i < \bar{\nu}_i$, $i = 1, 2, 3$, such that $A^{[\hat{\nu}]}$ has a pair of complex conjugate eigenvalues with modulus 1 which do not equal $\pm1, \pm\mathrm{i}, (-1 \pm \sqrt{3}\mathrm{i})/2$.
Fix $\nu_1 = \hat{\nu}_1$ and $\nu_3 = \hat{\nu}_3$. Set $\nu_2 = s$, and write $A^{[s]} := A^{[\nu]}$. Let $s_0 = \hat{\nu}_2$. Then $A^{[s]}$ admits a pair of complex conjugate eigenvalues with modulus 1 at $0 < s = s_0 < 1$. Thus $A^{[s]}$ has a pair of complex conjugate eigenvalues $w(s), \overline{w(s)}$ with $|w(s_0)| = 1$ for $s \in V$, where V is a small neighborhood of s_0. By Lemma 4.9, one has $\frac{d|w(s)|}{ds}|_{s=s_0} \neq 0$. Then the result can be proved in quite the same manner as the Theorem 4.3 in [33], so we omit it. □

Let $L_1(0) := Re(e^{-\mathrm{i}\theta_0}d(0))$, which is the first Lyapunov coefficient (see [38]). Using Theorem 4.5 and Theorem 4.6 in [37], we have the following.

Theorem 4.6. *Assume that the hypotheses of Theorem* 4.5 *hold. If* $L_1(0) \neq 0$*, then the family of maps* $\{T^{[\nu]} : 0 < \nu_i < \bar{\nu}_i, i = 1, 2, 3\}$ *admits a Neimark-Sacker bifurcation. Moreover, if* $L_1(0) < 0$*, a stable closed invariant curve bifurcates from the fixed point* p *while an unstable closed invariant curve bifurcates from the fixed point* p *if* $L_1(0) > 0$.

The biological interpretation of the condition $\det U_{\{i,j\}} < 0$ in Lemmas 4.7−4.8 and Theorems 4.5−4.6 is that at least one of the species i and j can resist invasion by the other in the absence of species k, whilst $\det U_{\{i,j\}} > 0$ means that at most one of the species i and j can resist invasion by the other in the absence of species k. Therefore, the biological meaning of the condition $\det U_{\{i,j\}}$, $i < j$, being not all of the same sign (say $\det U_{\{i,j\}} < 0$ and $\det U_{\{i,k\}} > 0$) is that at least one of the species i and j can resist invasion by the other in the absence of species k, whilst at most one of the species i and k can resist invasion by the other in the absence of species j.

Proposition 4.4. *Neimark-Sacker bifurcations can occur within each of classes* $26 - 31$.

Proof. In each of classes $26 - 31$, there exist mappings satisfying the hypotheses of Theorem 4.6; see Example 4.1 for definiteness. Noticing that the family of maps $\{T^{[\nu]} : 0 < \nu_i < \bar{\nu}_i, i = 1, 2, 3\}$ is contained in the same stable class by Remark 4.5, the result follows from Theorem 4.6 immediately. □

Example 4.1. Let

$$U^{[26]} = \begin{pmatrix} \frac{1}{2} & \frac{1}{4} & \frac{1}{4} \\ \frac{1}{8} & \frac{1}{8} & \frac{3}{4} \\ \frac{1}{3} & \frac{1}{6} & \frac{1}{2} \end{pmatrix}, \; U^{[27]} = \begin{pmatrix} \frac{3}{7} & \frac{3}{7} & \frac{1}{7} \\ \frac{3}{14} & \frac{3}{14} & \frac{4}{7} \\ \frac{4}{7} & \frac{1}{7} & \frac{2}{7} \end{pmatrix}, U^{[28]} = \begin{pmatrix} \frac{14}{39} & \frac{8}{13} & \frac{1}{39} \\ \frac{7}{13} & \frac{4}{13} & \frac{2}{13} \\ \frac{28}{39} & \frac{8}{39} & \frac{1}{13} \end{pmatrix},$$

$$U^{[29]} = \begin{pmatrix} \frac{36}{85} & \frac{33}{85} & \frac{16}{85} \\ \frac{18}{85} & \frac{66}{85} & \frac{1}{85} \\ \frac{6}{85} & \frac{77}{85} & \frac{2}{85} \end{pmatrix}, U^{[30]} = \begin{pmatrix} \frac{1}{24} & \frac{7}{8} & \frac{1}{12} \\ \frac{1}{16} & \frac{7}{16} & \frac{1}{2} \\ \frac{1}{12} & \frac{7}{12} & \frac{1}{3} \end{pmatrix}, U^{[31]} = \begin{pmatrix} \frac{9}{19} & \frac{2}{19} & \frac{8}{19} \\ \frac{9}{38} & \frac{12}{19} & \frac{5}{38} \\ \frac{6}{19} & \frac{8}{19} & \frac{5}{19} \end{pmatrix},$$

and $p = (1, 1, 1)$. Set $\bar{\nu}_j^{[i]} > 0$ which satisfies (12), $j = 1, 2, 3$, $i = 26, \cdots, 31$. Consider the map $T^{[i,\nu]} \in \mathrm{CRC}(3)$ with the parameters $U^{[i]}$ and $0 < \nu_j^{[i]} < \bar{\nu}_j^{[i]}$. Obviously, $T^{[i,\nu]}$ is in class i, and $\det U_{\{j,k\}}^{[i]}$, $j < k$, are not all of the same sign, $i = 26, \cdots, 31$. Furthermore, we have the following results by Theorem 4.6.

1. Set $i = 26$. Let $\nu_1 = s$, $\nu_2 = 1/9$, $\nu_3 = 1/3$, and $\nu = (\nu_1, \nu_2, \nu_3)$. It is easy to see that ν_i satisfy (12) when $0 < s < 1/3$, and hence the family of maps $\{T^{[i,\nu]} : 0 < s < 1/3\}$ is contained in class 26. It is not difficult to check that for $s = -\frac{489}{2717} + \frac{9\sqrt{71083}}{10868}$, $DT^{[i,\nu]}(p)$ has a pair of complex conjugate eigenvalues with modulus 1 which do not equal $\pm 1, \pm \mathrm{i}, (-1 \pm \sqrt{3}\mathrm{i})/2$. Furthermore, by calculating we obtain the first Lyapunov coefficient $L_1(0) = -8.003 \times 10^{-4} < 0$. Since the Lyapunov coefficient is a rather lengthy expression, the approximate value was computed as a *rational* by using MATLAB [38, 18]. Thus, by Theorem 4.6 there is a supercritical Neimark-Sacker bifurcation in class 26, i.e., a stable closed invariant curve bifurcates from the fixed point p; see Fig. 2.
2. Set $i = 27$. Let $\nu_1 = 2/7$, $\nu_2 = s$, $\nu_3 = 1/7$, and $\nu = (\nu_1, \nu_2, \nu_3)$. It is easy to see that ν_i satisfy (12) when $0 < s < 1/7$, and hence the family of maps $\{T^{[i,\nu]} : 0 < s < 1/7\}$ is contained in class 27. As $s = -\frac{25695}{16976} + \frac{49\sqrt{296929}}{16976}$, $DT^{[i,\nu]}(p)$ has a pair of complex conjugate eigenvalues with modulus 1 which do not equal $\pm 1, \pm \mathrm{i}, (-1 \pm \sqrt{3}\mathrm{i})/2$. The first Lyapunov coefficient is $L_1(0) = 1.04 \times 10^{-3} > 0$. So, class 27 can admit subcritical Neimark-Sacker bifurcations, i.e., there may exist unstable closed invariant curves in this class.
3. For $i = 28$, we let $\nu_1 = 1/3$, $\nu_2 = s$, $\nu_3 = 1/14$, and $\nu = (\nu_1, \nu_2, \nu_3)$. It is easy to see that ν_i satisfy (12) when $0 < s < 2/7$, and hence the family of maps $\{T^{[i,\nu]} : 0 < s < 2/7\}$ is contained in class 28. When $s = -\frac{10377985}{58635896} + \frac{39\sqrt{72964092217}}{58635896}$, $DT^{[i,\nu]}(p)$ has a pair of complex conjugate eigenvalues with modulus 1 which do not equal $\pm 1, \pm \mathrm{i}, (-1 \pm \sqrt{3}\mathrm{i})/2$. The first Lyapunov coefficient $L_1(0) = 3.697 \times 10^{-5} > 0$. Thus, by Theorem 4.6 there is a subcritical Neimark-Sacker bifurcation in class 28, i.e., an unstable closed invariant curve bifurcates from the fixed point

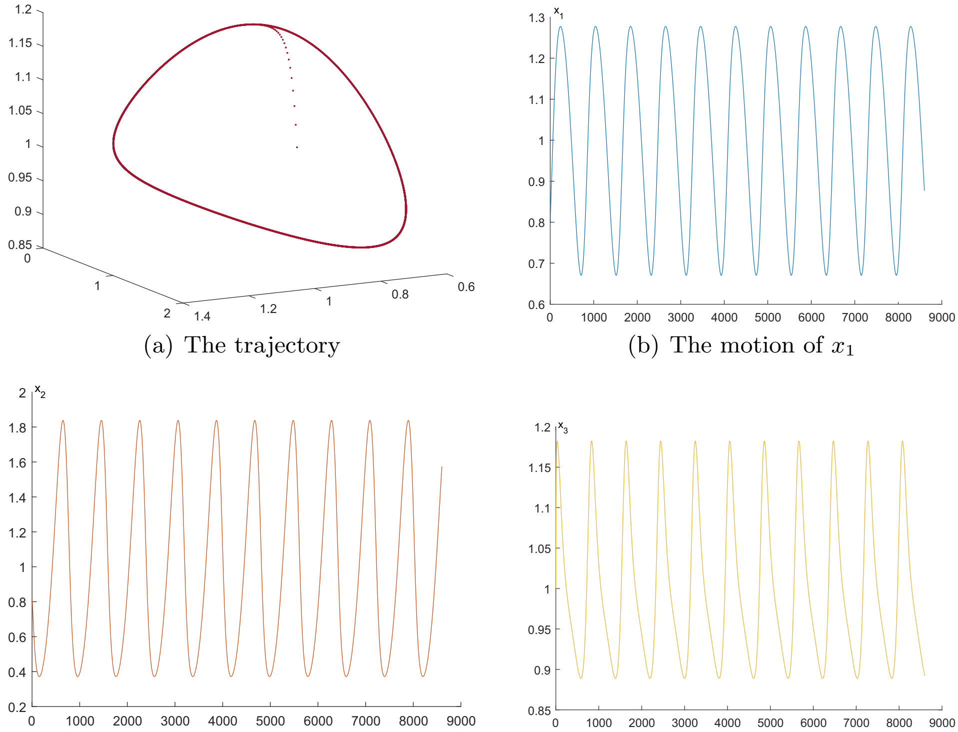

(a) The trajectory (b) The motion of x_1

(c) The motion of x_2 (d) The motion of x_3

Figure 2: The trajectory emanating from $x_0 = (0.8, 0.8, 1)$ for the map $T \in \mathrm{CRC}(3)$ with the parameters U^{26} given in Example 4.1 and $\nu_1 = 0.04$, $\nu_2 = \frac{1}{9}$, $\nu_3 = \frac{1}{3}$ tends to an attracting closed invariant curve, $i = 1, 2, 3$.

p.

4. For $i = 29$, we let $\nu_1 = 7/17$, $\nu_2 = s$, $\nu_3 = 1/43$, and $\nu = (\nu_1, \nu_2, \nu_3)$. It is easy to see that ν_i satisfy (12) when $0 < s < 13/17$, and hence the family of maps $\{T^{[i,\nu]} : 0 < s < 13/17\}$ is contained in class 29. When $s = -\frac{22152020138}{173689341859} + \frac{170\sqrt{17064477965620957}}{173689341859}$, $DT^{[i,\nu]}(p)$ has a pair of complex conjugate eigenvalues with modulus 1 which do not equal $\pm 1, \pm \mathrm{i}, (-1 \pm \sqrt{3}\mathrm{i})/2$. The first Lyapunov coefficient $L_1(0) = 1.843 \times 10^{-7} > 0$. So, class 29 can admit subcritical Neimark-Sacker bifurcations, i.e., there may exist unstable closed invariant curves in this class.

5. For $i = 30$, we set $\nu_1 = 1/25$, $\nu_2 = s$, $\nu_3 = 1/4$, and $\nu = (\nu_1, \nu_2, \nu_3)$. It is easy to see that ν_i satisfy (12) when $0 < s < 3/8$, and hence the family of maps $\{T^{[i,\nu]} : 0 < s < 3/8\}$ is contained in class 30. As $s = -\frac{786572}{8573383} + \frac{48\sqrt{278933069}}{8573383}$, $DT^{[i,\nu]}(p)$ has a pair of complex conjugate eigenvalues with modulus 1 which do not equal $\pm 1, \pm \mathrm{i}, (-1 \pm \sqrt{3}\mathrm{i})/2$. The first Lyapunov coefficient $L_1(0) = 1.138 \times 10^{-5} > 0$. So, class 30 can admit subcritical Neimark-Sacker bifurcations, i.e., there may exist unstable closed invariant curves in this class.

6. For $i = 31$, we set $\nu_1 = 3/7$, $\nu_2 = s$, $\nu_3 = 1/4$, and $\nu = (\nu_1, \nu_2, \nu_3)$. It is easy to see that ν_i satisfy (12) when $0 < s < 3/5$, and hence the family of maps $\{T^{[i,\nu]} : 0 < s < 3/5\}$ is contained in class 31. As $s = -\frac{3841937}{14371150} + \frac{19\sqrt{42841117729}}{14371150}$, $DT^{[i,\nu]}(p)$ has a pair of complex conjugate eigenvalues with modulus 1 which do not equal $\pm 1, \pm \mathrm{i}, (-1 \pm \sqrt{3}\mathrm{i})/2$. The first Lyapunov coefficient $L_1(0) = -5.691 \times 10^{-4} < 0$. By Theorem 4.6 we know that there is a supercritical Neimark-Sacker bifurcation in class 31, i.e., a stable closed invariant curve bifurcates from the fixed point p; see Fig. 3.

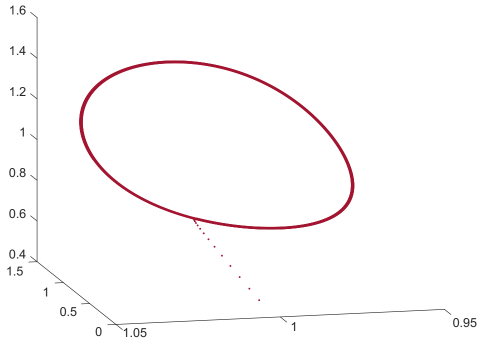

(a) The trajectory

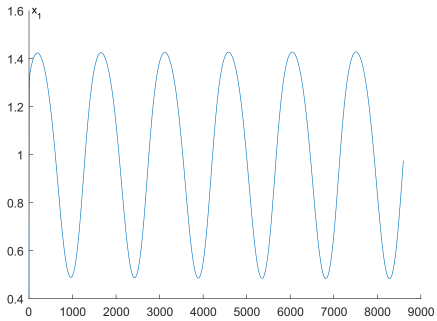

(b) The motion of x_1

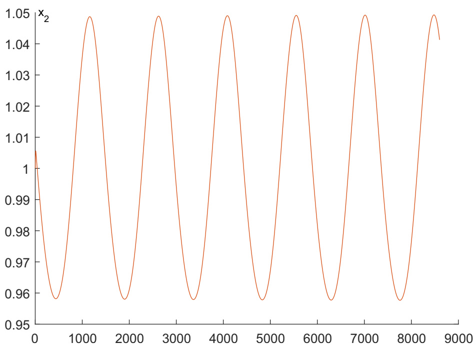

(c) The motion of x_2

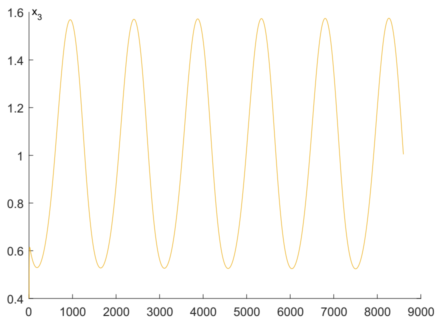

(d) The motion of x_3

Figure 3: The trajectory emanating from $x_0 = (0.4, 1, 0.4)$ for the map $T \in \mathrm{CRC}(3)$ with the parameters U^{31} given in Example 4.1 and $\nu_1 = \frac{3}{7}$, $\nu_2 = 0.006$, $\nu_3 = \frac{1}{4}$ tends to an attracting closed invariant curve, $i = 1, 2, 3$.

Remark 4.6. *Roeger [46] studied the Neimark-Sacker bifurcations for the special 3D Ricker maps* (10) *with $\nu_1 = \nu_2 = \nu_3$ and μ_{ij} satisfying the conditions of class 27 in Table A.1, and it was shown that non-degenerate Neimark-Sacker bifurcations can occur in this case. Example 4.1 shows that non-degenerate Neimark-Sacker bifurcations can also occur when ν_1, ν_2, ν_3 are not identical. Moreover, for 3D Ricker maps* (10)*, non-degenerate Neimark-Sacker bifurcations can occur* *even when μ_{ij} satisfy the conditions of classes 26 and 28–31 in Table A.1.*

Consider a sufficiently smooth map $\Phi(x,\beta) : \mathbb{R}^n \times \mathbb{R}^2 \to \mathbb{R}^n$, where $x \in \mathbb{R}^n, \beta \in \mathbb{R}^2$. Assume that Φ has a fixed point $x = 0$ at $\beta = 0$ for which the Neimark-Sacker bifurcation conditions hold. Thus $D\Phi(0,0)$ has a pair of conjugate complex eigenvalues lying on the unit circle. Assume further that Φ satisfies some other non-degeneracy conditions such that the restriction of Φ to the two dimensional center manifold at the critical parameter value $\beta = 0$ can be transformed to the normal form in polar coordinates (ϱ,θ) (see [37] for more details):

$$\begin{cases} \varrho \mapsto \varrho + \mu_1\varrho + \mu_2\varrho^3 + L_2(\mu)\varrho^5 + \cdots, \\ \theta \mapsto \theta + \vartheta(\mu) + \upsilon(\mu,\varrho)\varrho^2 + \cdots, \end{cases}$$

where $\mu = (\mu_1,\mu_2)$ and the dots denote terms of higher order in ϱ and θ. Truncating the higher order terms gives the map

$$\begin{cases} \varrho \mapsto \varrho + \mu_1\varrho + \mu_2\varrho^3 + L_2(\mu)\varrho^5, \\ \theta \mapsto \theta + \vartheta(\mu) + \upsilon(\mu,\varrho)\varrho^2. \end{cases} \tag{22}$$

$\varrho = 0$ corresponds to the fixed point of the system and any positive fixed point of the ϱ-map in (22) corresponds to a closed invariant curve in phase space. $\mu_1 = 0$ corresponds to the Neimark-Sacker bifurcation curve, for which a pair of conjugate complex eigenvalues lie on the unit circle, and μ_2 is the corresponding first Lyapunov coefficient when $\mu_1 = 0$. For $\mu_2 < 0$, a supercritical Hopf bifurcation occurs at $\mu_1 = 0$, whereas for $\mu_2 > 0$ a subcritical Hopf bifurcation occurs at $\mu_1 = 0$. For $\mu_2 = 0$ the Neimark-Sacker bifurcation becomes degenerate, which is called the Chenciner bifurcation (see Kuznetsov [37] and Gaunersdorfer *et al.* [13]). The Chenciner bifurcation occurs at $\mu_1 = 0$ for which a pair of conjugate complex eigenvalues lie on the unit circle and the first Lyapunov coefficient $\mu_2 = 0$. An extra non-degeneracy condition for the Chenciner bifurcation is $L_2(0) \neq 0$. Here we show some details by assuming that $L_2(0) < 0$. Without loss of generality, assume that $L_2(0) = -1$.

ϱ^* is positive fixed point of the ϱ-map in (22) iff it is a positive solution to the equation $\mu_1 + \mu_2\varrho^2 - \varrho^4 = 0$, i.e.,

$$(\varrho^2 - \frac{\mu_2}{2})^2 = \frac{\mu_2^2}{4} + \mu_1. \tag{23}$$

When $\mu_1 > 0$ there is exactly one positive solution for equation(23). For $\mu_1 < 0$, equation (23) has no solution when $\frac{\mu_2^2}{4} + \mu_1 < 0$, while equation (23) has two distinct positive solutions when $\frac{\mu_2^2}{4} + \mu_1 > 0$, $\mu_1 < 0$ and $\mu_2 > 0$ (in this case, the outer closed invariant curve is stable, while the inner one is unstable). For μ lying on the curve $T_c := \{\mu : \frac{\mu_2^2}{4} + \mu_1 = 0, \mu_2 > 0\}$, equation (23) has two equal

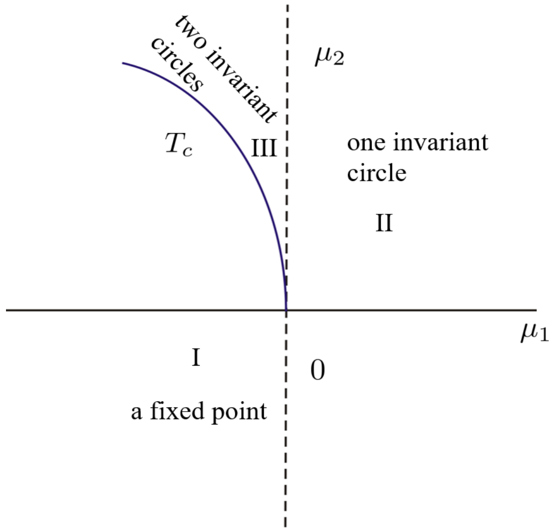

Figure 4: Bifurcation diagram of the Chenciner bifurcation in the (μ_1, μ_2)-plane for the case $L_2(0) < 0$. The origin is the Chenciner bifurcation point. The vertical dashed line $\mu_1 = 0$ is the Neimark-Sacker bifurcation curve. In the region I below the curve T_c, there is only one fixed point which is stable; in the region II ($\mu_1 > 0$), there is a unique closed invariant curve which is stable; in the region III between the curve T_c and the positive μ_2-axis, a stable closed invariant curve (outer) and an unstable closed invariant curve (inner) coexist; on the solid curve T_c, these two circles coincide.

positive solutions (in this case, the unstable and stable closed invariant curves approach each other). See Fig. 4 for a sketch of this bifurcation diagram. For $L_2(0) > 0$, it can be treated similarly, and in this case, the outer closed invariant curve is unstable, while the inner one is stable.

The Chenciner bifurcation is a two-parameter bifurcation phenomenon of a fixed point. Although the normal form computations for Chenciner bifurcations are straightforward, in practical models they can be very complicated. Based on the numerical methods provided in [18], we give an example by using MATLAB [38, 19] to show that the Ricker map (16) in class 29 can admit Chenciner bifurcations, so in this class, two isolated closed invariant curves can coexist. See Example 4.2.

Example 4.2. Consider the parameters $U^{[29]}$ given in Example 4.1. Let $\nu_3 = \frac{1}{43}$, $0 < \nu_1 < \frac{7}{17}, 0 < \nu_2 < \frac{13}{17}$, and $\nu = (\nu_1, \nu_2, \nu_3)$. By numerical calculation, we find that the two-parameter map $T^{[29,\nu]}$ with the coefficients $U^{[29]}$ and ν has a Chenciner bifurcation point at $p = (1, 1, 1)$ when $\nu_1 = 0.034559$ and $\nu_2 = 0.000368$. The normal form coefficient $L_2(0) = -1.1233 \times 10^{-6} < 0$, so a large stable closed invariant curve surrounding a small unstable closed invariant curve can occur in class 29.

Suppose that the 3-dimensional map T has a carrying simplex Σ, which is homeomorphic to Δ^2. Suppose further that $q_{\{1\}} = (q_1, 0, 0)$, $q_{\{2\}} = (0, q_2, 0)$ and $q_{\{3\}} = (0, 0, q_3)$ are its three axial fixed points lying on the vertices of Σ. If each $q_{\{i\}}$ is a saddle, and $\partial\Sigma \cap \pi_i$ is the saddle connection between $q_{\{j\}}$ and $q_{\{k\}}$, then T admits a heteroclinic cycle of May-Leonard type: $q_{\{1\}} \to q_{\{2\}} \to q_{\{3\}} \to q_{\{1\}}$ (or the arrows reserved), which is just the boundary of Σ. For this case, we can obtain the stability of the heteroclinic cycle $\partial\Sigma$ by the result in [34].

Lemma 4.10 (Theorem 3 in [34])**.** *Suppose that $\partial\Sigma$ is a heteroclinic cycle above. Then the heteroclinic cycle $\partial\Sigma$ repels (attracts) if*

$$\prod_{i=1}^{3} \ln G_i(q_{\{i-1\}}) + \prod_{i=1}^{3} \ln G_i(q_{\{i+1\}}) > 0 \ (< 0),$$

where $i \in \{1, 2, 3\}$ is considered cyclic.

Note that for any map T in class 27, each axial fixed point $q_{\{i\}}$ is a saddle on Σ, and $\partial\Sigma \cap \pi_i$ is the heteroclinic connection between $q_{\{j\}}$ and $q_{\{k\}}$, where i, j, k are distinct. So $\partial\Sigma$ forms a heteroclinic cycle of May-Leonard type: $q_{\{1\}} \to q_{\{2\}} \to q_{\{3\}} \to q_{\{1\}}$ (or the arrows reserved), i.e., any map T in class 27 possesses a heteroclinic cycle (see Table A.1 (27)). By Lemma 4.10 one can obtain Proposition 4.5 immediately; see also [26] for a similar result.

Set $w_{ij} = \nu_j(1 - \mu_{ji}/\mu_{ii})$, where $i \neq j$. Let $\vartheta = w_{12}w_{23}w_{31} + w_{21}w_{13}w_{32}$.

Proposition 4.5. *Assume that $T \in \mathrm{CRC}(3)$ is in class 27. If $\vartheta < 0$ (> 0), then the heteroclinic cycle $\partial\Sigma$ of T attracts (repels).*

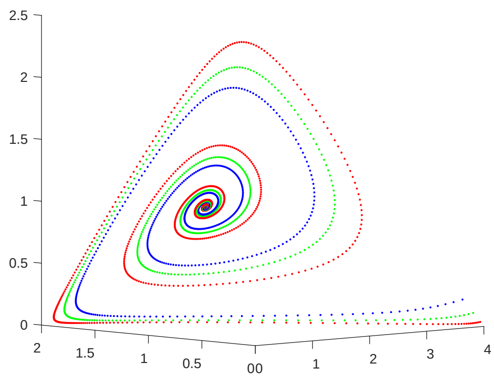

Figure 5: The trajectories emanating from $x_0 = (4, 0.03, 0.03)$, $x_0 = (4, 0.1, 0.1)$ and $x_0 = (4, 0.2, 0.2)$ for the map $T \in \mathrm{CRC}(3)$ in Example 4.3 lead away from $\partial\Sigma$ and tend to the positive fixed point p.

Example 4.3. Let $U = \begin{pmatrix} \frac{1}{4} & \frac{7}{12} & \frac{1}{6} \\ \frac{1}{12} & \frac{1}{2} & \frac{5}{12} \\ \frac{1}{3} & \frac{1}{3} & \frac{1}{3} \end{pmatrix}$ and $\nu_1 = \frac{1}{5}, \nu_2 = \frac{1}{5}, \nu_3 = \frac{1}{5}$. Consider the map $T \in \mathrm{CRC}(3)$ with the parameters U and ν_i, $i = 1, 2, 3$. It is easy to check that T belongs to class 27 with $\vartheta > 0$. It then follows from Proposition 4.5 that the heteroclinic cycle $\partial\Sigma$ repels for T and see also the numerical experiment in Fig. 5.

Let $\hat{U} = \begin{pmatrix} 1 & 2 & \frac{1}{2} \\ \frac{1}{2} & 1 & 2 \\ 2 & \frac{1}{2} & 1 \end{pmatrix}$ and $\hat{\nu}_1 = \frac{1}{7}, \hat{\nu}_2 = \frac{1}{7}, \hat{\nu}_3 = \frac{1}{7}$. Consider the map $\hat{T} \in \mathrm{CRC}(3)$ with the parameters $\hat{U}$ and $\hat{\nu}_i$, $i = 1, 2, 3$. It is easy to check that $\hat{T}$ belongs to class 27 with $\vartheta < 0$. It then follows from Proposition 4.5 that the heteroclinic cycle $\partial\Sigma$ attracts for $\hat{T}$ and see also the numerical experiment in Fig. 6.

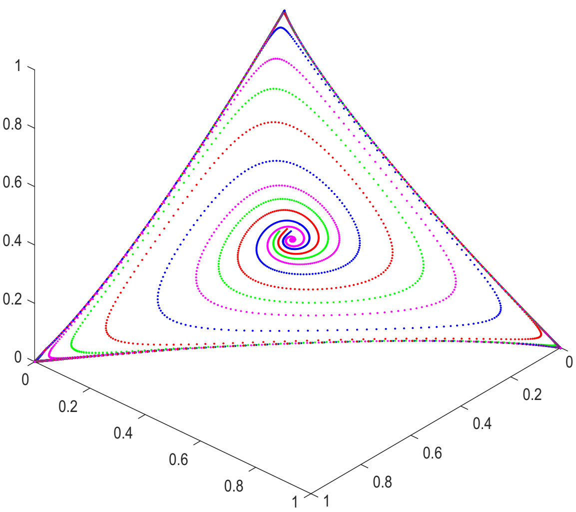

Figure 6: The trajectories emanating from $x_0 = (0.8667, 0.8667, 1)$, $x_0 = (0.9, 0.9, 1)$, $x_0 = (0.9333, 0.9333, 1)$ and $x_0 = (1, 1, 1)$ for the map $\hat{T} \in \mathrm{CRC}(3)$ in Example 4.3 approach to $\partial\Sigma$.

Remark 4.7. *Consider the competitive continuous-time Lotka-Volterra system*

$$\frac{dx_i}{dt} = x_i(\nu_i(1 - \sum_{j=1}^{3} \mu_{ij} x_j)), \ \ \nu_i, \mu_{ij} > 0, i, j = 1, 2, 3. \tag{24}$$

System (24) *admits a heteroclinic cycle:* $q_{\{1\}} \to q_{\{2\}} \to q_{\{3\}} \to q_{\{1\}}$ *when the* *parameters satisfy*

$$\gamma_{12} > 0, \gamma_{13} < 0, \gamma_{21} < 0, \gamma_{23} > 0, \gamma_{31} > 0, \gamma_{32} < 0, \tag{25}$$

i.e. when the Ricker map (16) *admits one; see class* 27 *in Table A.1. According to [27], we know that for system* (24) $\partial\Sigma$ *attracts if* $\vartheta < 0$, *while repels if* $\vartheta > 0$, *where* ϑ *is defined above. By Proposition 4.5, one can see that the criteria on the stability of heteroclinic cycles for the Lotka-Volterra system* (24) *and Ricker map* (16) *are the same; see also [34].*

Let $U = \begin{pmatrix} \frac{3}{7} & \frac{2}{7} & \frac{1}{7} \\ \frac{3}{14} & \frac{3}{14} & \frac{4}{7} \\ \frac{1}{2} & \frac{1}{7} & \frac{2}{7} \end{pmatrix}$ *and* $\nu_1 = \frac{1}{10}, \nu_2 = \frac{1}{7}, \nu_3 = \frac{1}{7}$. *Note that* (12) *and* (25) *hold for such* μ_{ij} *and* ν_i. *Consider the Ricker map* (16) *and system* (24) *with the parameters* μ_{ij} *and* ν_i, *respectively,* $i = 1, 2, 3$. *Then the Ricker map* (16) *(resp. the Lotka-Volterra system* (24)*) admits a heteroclinic cycle* $\partial\Sigma$ *(resp.* $\partial\hat{\Sigma}$, *where* $\hat{\Sigma}$ *is the carrying simplex for* (24)*; see [62]). It is easy to check that* $\vartheta > 0$. *So the heteroclinic cycles* $\partial\Sigma$, $\partial\hat{\Sigma}$ *repels for* (16) *and* (24), *respectively. Besides,* $p = (\frac{70}{61}, \frac{84}{61}, \frac{49}{61})$ *is a repelling positive fixed point for both* (16) *and* (24). *Then according to Poincaré-Bendixson theorem, there is a limit cycle* Γ *contained in the interior of* $\hat{\Sigma}$ *surrounding* p *for Lotka-Volterra system* (24)*; see Fig. 7 for the numerical experiment. However, Poincaré-Bendixson theorem does not hold*

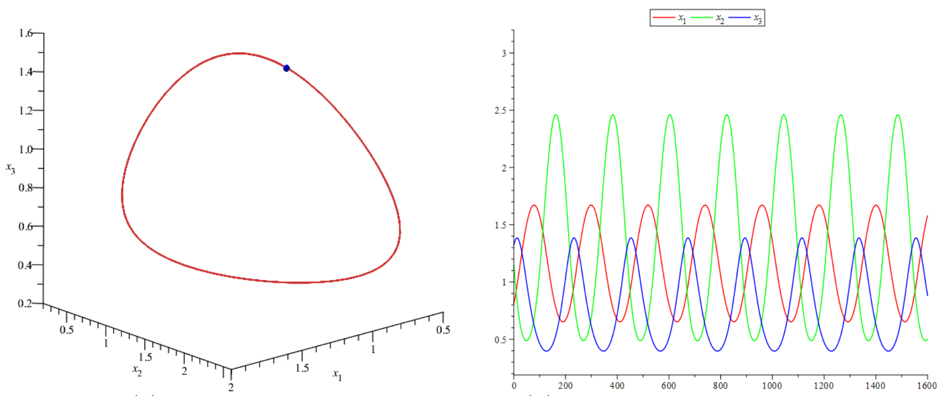

(a) The trajectory (b) The motion of each component

Figure 7: The orbit emanating from $x_0 = (0.81, 1.15, 1.32)$ for system (24) with parameters μ_{ij} and ν_i given in Remark 4.7 tends to a limit cycle, where the blue point on the cycle is x_0.

for discrete-time systems. So we do numerical experiments and find that there exists an attracting closed invariant curve in this domain; see Fig. 8. Thus, we conclude the following conjecture.

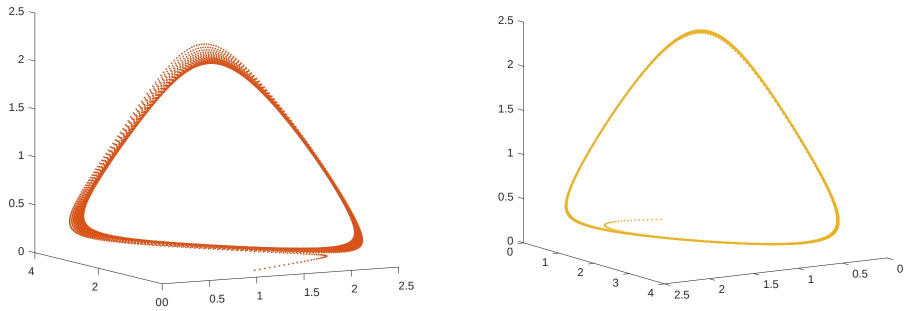

(a) The orbit with $x_0 = (1, 0.0667, 0.0667)$ (b) The orbit with $x_0 = (1, 0.1, 0.1)$

Figure 8: The orbits emanating from $x_0 = (1, 0.0667, 0.0667)$ and $x_0 = (1, 0.1, 0.1)$ for the Ricker map (16) with parameters μ_{ij} and ν_i given in Remark 4.7 tend to an invariant closed curve.

Conjecture. For the Ricker map $T \in \mathrm{CRC}(3)$ which is in class 27, there exists an attracting (repelling) invariant closed curve contained in $\dot{\Sigma} \setminus \{p\}$ if both the heteroclinic cycle $\partial\Sigma$ and p are repelling (attracting).

5. The occurrence of chaos

In this section, we study the possible routes to chaos for Ricker maps (10). Specifically, we show that the carrying simplex disappears as the growth rates increase while chaos occurs by concrete examples. A 4D Ricker map which possesses a carrying simplex containing a chaotic attractor is also given.

5.1. Carrying simplex breaks and chaos appears

We first recall the 1D Ricker map

$$T(x) = xe^{r(1-x)}, \tag{26}$$

where $x \geq 0$ and $r > 0$. For $0 < r \leq 2$, the positive fixed point $x = 1$ is globally attracting, i.e. $x = 1$ is the carrying simplex, while for $r > 2$, carrying simplex breaks. Indeed, noticing that $T'(1) = 1 - r$, a period-doubling bifurcation occurs at $r = 2$ and a cascade of further period-doubling bifurcations appear as r increases, yielding 2-periodic points, 4-periodic points, 8-periodic points, …, until about $r \approx 2.6924$, where the dynamics becomes chaotic; see [41] for more details. To follow these dynamic scenarios, we generate a Bifurcation Diagram for $0 < r \leq 4.5$ as shown in Fig. 9, where the choice of initial value is $x_0 = 1.2$.

Consider the 2D Ricker map T given by

$$\begin{aligned} T_1(x_1, x_2) &= x_1(\exp(r(1 - x_1 - \tfrac{1}{8}x_2))), \\ T_2(x_1, x_2) &= x_2(\exp(\tfrac{1}{2}(1 - \tfrac{1}{2}x_1 - x_2))), \end{aligned} \tag{27}$$

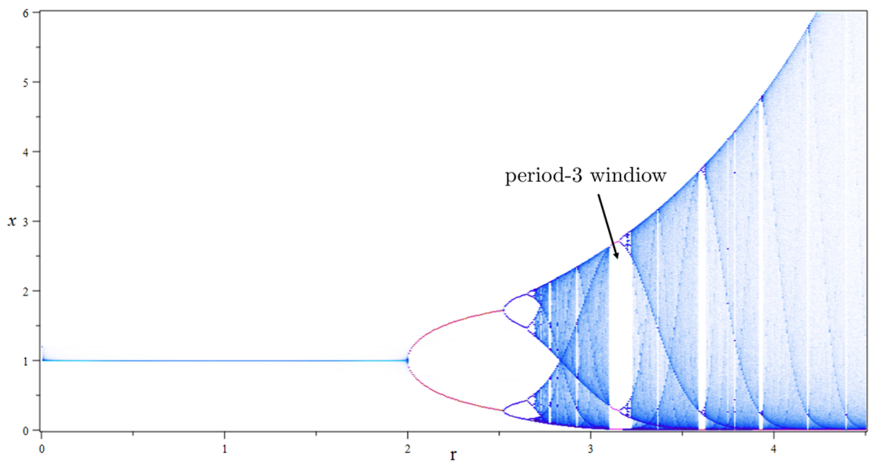

Figure 9: The bifurcation diagram of the Ricker map (26).

where $(x_1, x_2) \in \mathbb{R}^2_+$ and $r > 0$. System (27) has three boundary fixed points: 0, $q_{\{1\}} = (1, 0)$, $q_{\{2\}} = (0, 1)$ which are all unstable for any $r > 0$, and a unique positive fixed point $p = (\frac{14}{15}, \frac{8}{15})$. When $r < \frac{8}{9}$, the condition (12) holds, so system (27) admits a carrying simplex, and p is globally attracting on $\dot{\mathbb{R}}^2_+$. Since the carrying simplex for the 1D Ricker map (26) breaks when $r > 2$, it also disappears for system (27) when $r > 2$. Indeed, any kind of nontrivial dynamics breaks the carrying simplex for 2D system (27). Our aim here is to study the evolution of the attractor as $r > 2$ varies for system (27).

The results of numerical investigation are reported here. When $r = \frac{104}{49}$, p has an eigenvalue -1, and a period-doubling bifurcation occurs. An attracting 2-periodic orbit is detected at $r = 2.2$; see Table 1(a). As r is increased, these periodic points also undergo period-doubling bifurcations followed by a cascade of further period-doubling bifurcations; see Table 1(b)-(c) for the 4-periodic orbit and 8-periodic orbit. Such period-doubling cascades eventually lead to chaos at $r \approx 2.875$; see Table 1(d)-(e) and (g)-(h) for these chaotic attractors. Note that as r increases, there are still some ranges such that periodic orbits appear again, and at $r = 3.35$, a 3-periodic orbit is detected; see Table 3(f).

Table 1: Evolution of the attractor for system (27) as r increases from 2.2 to 4. The initial value used is $x_0 = (0.3, 1.1)$.

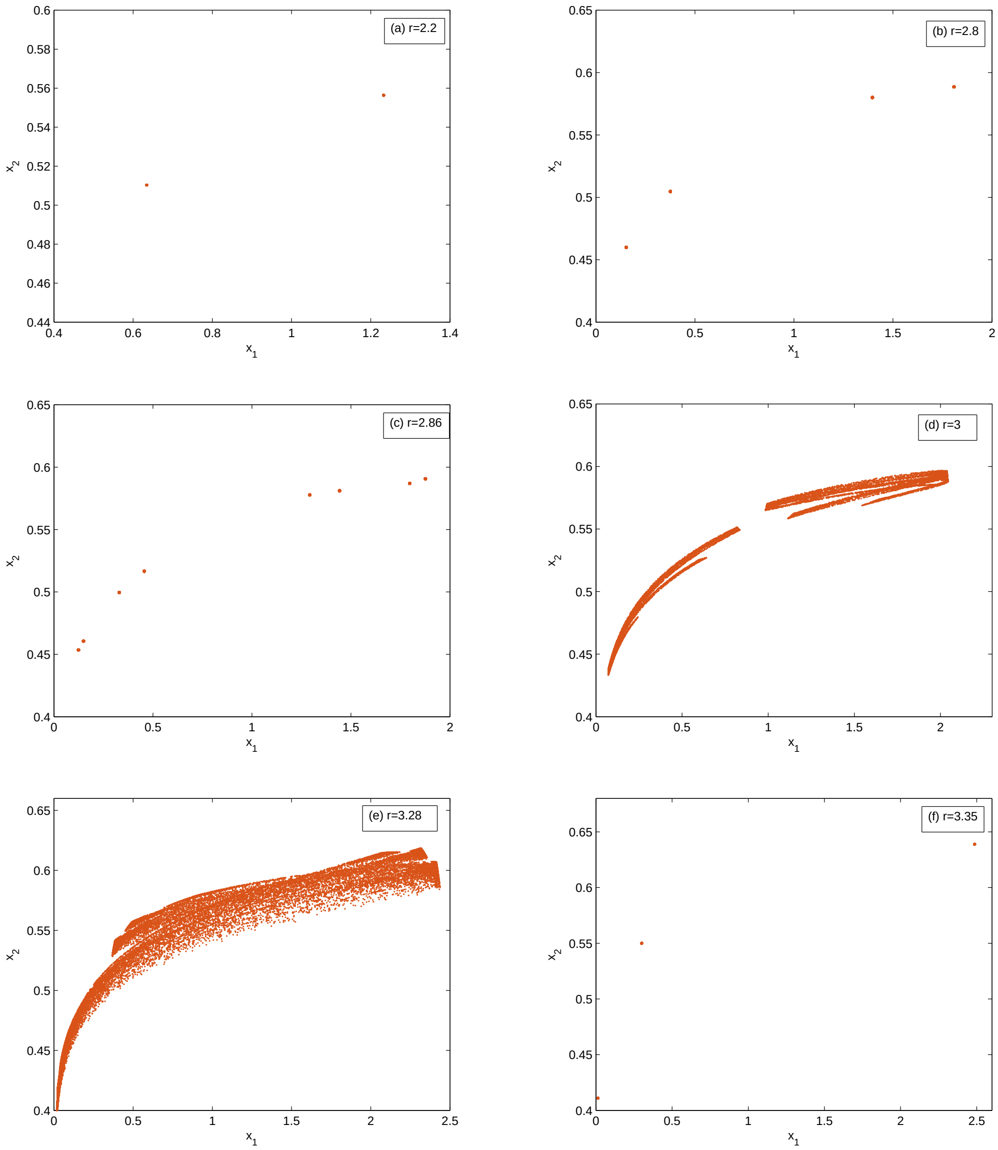
(a) r=2.2
(b) r=2.8
(c) r=2.86
(d) r=3
(e) r=3.28
(f) r=3.35
x1
x2

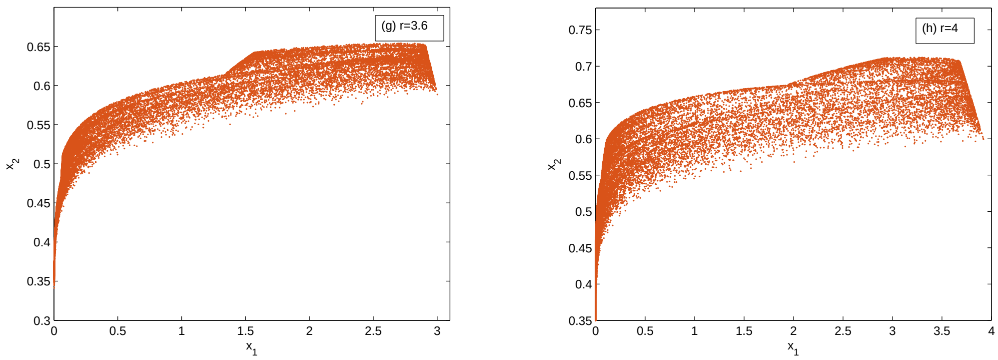

See also [31] for a detailed study of bifurcations of periodic points for 2D Ricker models (17) of symmetric competition.

Consider the 3D Ricker map T given by

$$\begin{aligned} T_1(x_1,x_2,x_3) &= x_1(\exp(r(1-x_1-\tfrac{1}{8}x_2-\tfrac{1}{2}x_3))), \\ T_2(x_1,x_2,x_3) &= x_2(\exp(\tfrac{1}{3}(1-\tfrac{1}{2}x_1-x_2-\tfrac{1}{2}x_3))), \\ T_3(x_1,x_2,x_3) &= x_3(\exp(\tfrac{1}{4}(1-\tfrac{1}{2}x_1-\tfrac{1}{4}x_2-x_3))), \end{aligned} \tag{28}$$

where $(x_1,x_2,x_3)\in\mathbb{R}^3_+$ and $r>0$.

There are seven boundary fixed points: 0, $q_{\{1\}}=(1,0,0)$, $q_{\{2\}}=(0,1,0)$, $q_{\{3\}}=(0,0,1)$, $v_{\{1\}}=(0,\frac{4}{7},\frac{6}{7})$, $v_{\{2\}}=(\frac{2}{3},0,\frac{2}{3})$, $v_{\{3\}}=(\frac{14}{15},\frac{8}{15},0)$, which are all unstable for any $r>0$, and a unique positive fixed point $p=(\frac{2}{3},\frac{8}{21},\frac{4}{7})$. When $r<\frac{8}{13}$ the condition (12) holds, so system (28) admits a carrying simplex, which belongs to stable class 33; see Table A.1(33). Recall also that the carrying simplex for the 1D Ricker map (26) disappears when $r>2$, it also breaks for system (28) when $r>2$. As r increases, cascades of period-doubling bifurcations can also occur which lead to chaos.

At $r=\frac{876}{299}$, p undergos a period-doubling bifurcation followed by a cascade of period-doubling bifurcations. See Table 2(a)-(b) for the 2-periodic orbit and 4-periodic orbit. The period-doubling cascades lead to chaos at about $r=4.02$; see Table 2(c), (e) and (f) for the chaotic attractors. As r increases, periodic orbits also appear and at $r=4.75$, a 3-periodic orbit is detected; see Table 3(d).

Table 2: Evolution of the attractor for system (28) as r increases from 2.95 to 5.2. The initial value used is $x_0 = (0.3, 1.1, 0.3)$.

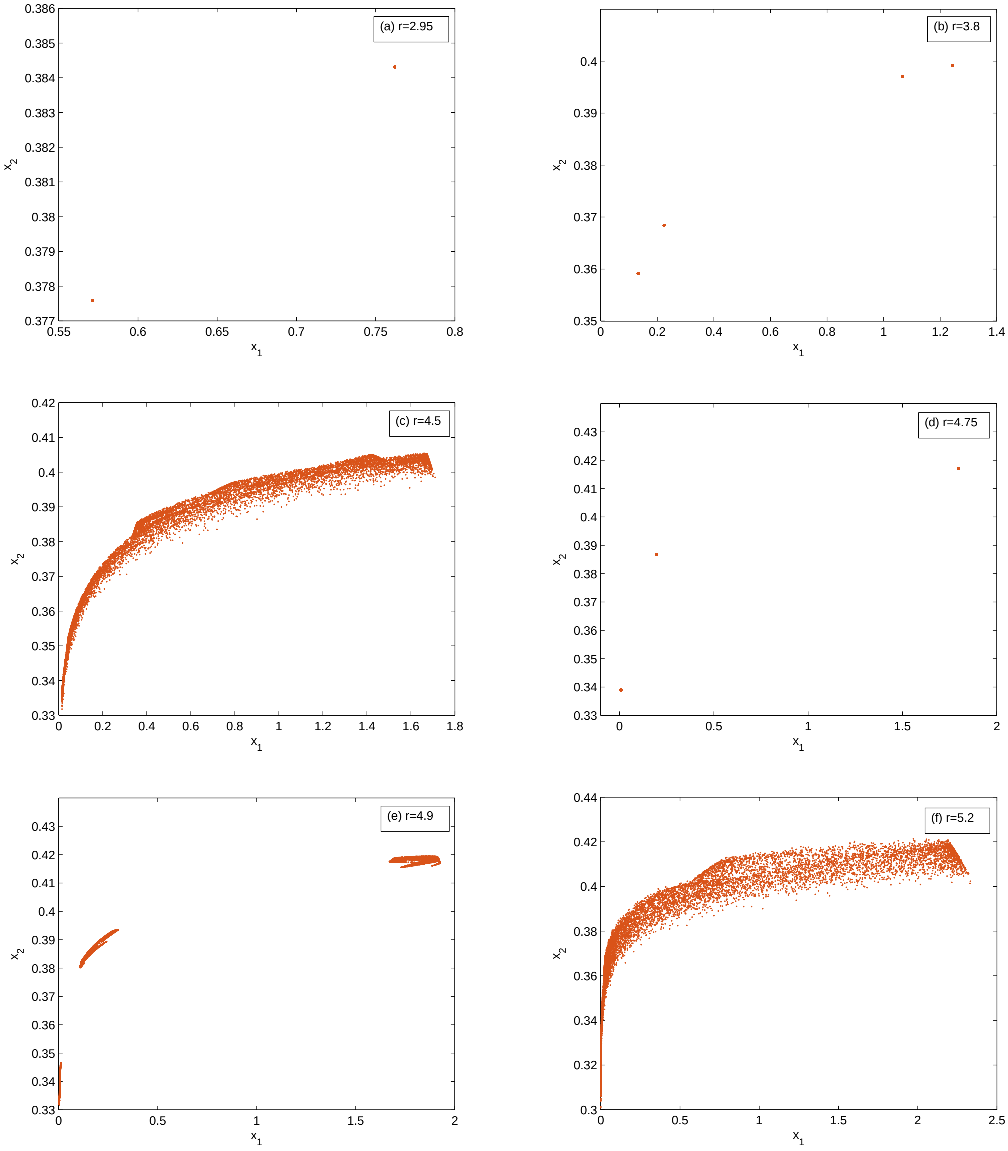

5.2. Chaotic attractor in the carrying simplex

In this subsection, we construct an example to show that chaos can occur in the carrying simplex. In this example, we numerically find that there are two routes to chaos, that is

- quasiperiod-doubling cascades lead to chaos;
- cascades of homoclinic-doubling bifurcations lead to chaos.

Quasiperiod-doubling bifurcation in our context is referred to the phenomenon that a quasiperiodic curve rounding twice bifurcates from the original one. We call the bifurcated quasiperiodic curve a 2-quasiperiodic curve. The phenomena, quasiperiod-doubling cascades leading to chaos, have been observed in [12, 55]. Homoclinic-doubling bifurcation in this context is referred to the phenomenon that a homoclinic connection rounding twice bifurcates from the original one; see [36] and references therein for the definition and historical background in continuous-time systems. Also, we call the bifurcated homoclinic connection a 2-homoclinic connection.

Consider the one-parameter family of 4D Ricker maps defined on $\mathbb{R}^4_+$:

$$\begin{aligned} T_1(x) &= x_1 \exp(0.178(1 - 1.821x_1 - 0.898x_2 - 0.774x_3 - 3.452x_4)), \\ T_2(x) &= x_2 \exp(0.222(1 - 0.912x_1 - 2.289x_2 - 0.0032x_3 - 6.641x_4)), \\ T_3(x) &= x_3 \exp(0.105(1 - 2.321x_1 - 0.994x_2 - 1.507x_3 - 0.0669x_4)), \\ T_4(x) &= x_4 \exp(r(1 - 0.0425x_1 - 3.541x_2 - 1.691x_3 - 2.342x_4)), \end{aligned} \tag{29}$$

where $x = (x_1, x_2, x_3, x_4) \in \mathbb{R}^4_+$ and $r > 0$. It is easy to check that system (29) has nine boundary fixed points: the trivial fixed point 0; four axial fixed points $q_{\{1\}}, q_{\{2\}}, q_{\{3\}}, q_{\{4\}}$ with $q_{\{i\}}$ lying on x_i-axis; three planar fixed points $v_{\{1,2\}}, v_{\{2,3\}}, v_{\{2,4\}}$ with $v_{\{i,j\}}$ lying on the positive cone of the (x_i, x_j) plane; a fixed point $w^{\{2\}}$ on the interior of π_2, which are all unstable, and a unique positive fixed point $p \approx (0.204956, 0.076478, 0.293204, 0.095932)$.

When $0 < r < 0.3074$, condition (12) holds, and hence system (29) admits a carrying simplex Σ. All nontrivial fixed points are on Σ, and the boundary fixed points are on $\partial\Sigma$.

At $r \approx 0.016974$, the positive fixed point undergoes a supercritical Neimark-Sacker bifurcation with first Lyapunov coefficient $L_1(0) = -0.03156 < 0$, which was computed as a rational by using MATLAB [18, 19]. So, a stable closed invariant curve arises for $r > 0.016974$. We now study the evolution of the attractor on Σ for increasing r over the range $0.016974 < r < 0.3074$.

A quasiperiodic curve is detected when $r = 0.03$ (Table 3(a)). The quasiperiodic curve increases in size as r is increased, until about $r = 0.0364$, where a quasiperiod-doubling cascade begins; see Table 3(b)-(d) for the 2-quasiperiodic curve, 4-quasiperiodic curve and 8-quasiperiodic curve. Such quasiperiod-doubling cascades eventually lead to chaos; see Table 3(e)-(g) for the chaotic attractors, which are very like the Rössler attractor in the continuous-time system [48]. Note that as r increases, there are still some ranges such that quasiperiodic curves appear again, and at $r = 0.0483$, a 3-quasiperiodic curve occurs (Table 3(h)). When $r > 0.049$, the chaotic attractor persists, and becomes a almost filled-in chaotic attractor at $r = 0.061$; see Table 3(i)-(j).

Table 3: Evolution of the attractor in the carrying simplex for system (29) as r increases from 0.03 to 0.061. Quasiperiodic doubling cascades lead to chaos. The initial value used is $x_0 = (0.4, 0.3, 0.4, 0.5)$.

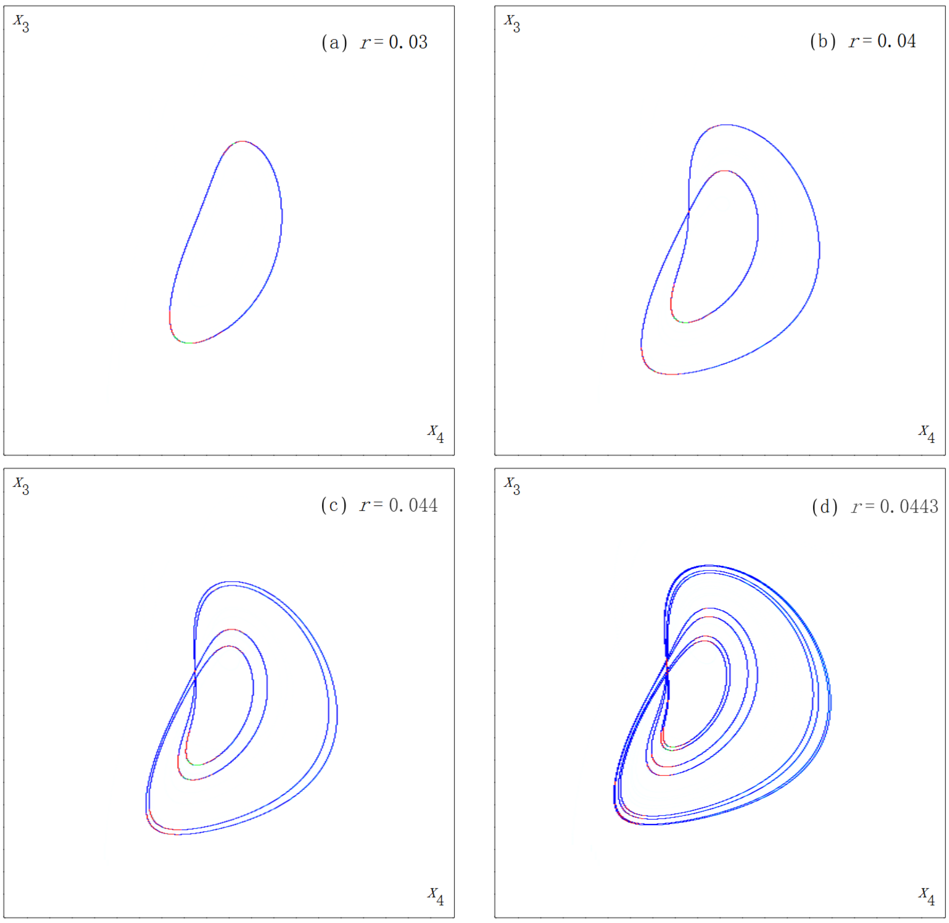

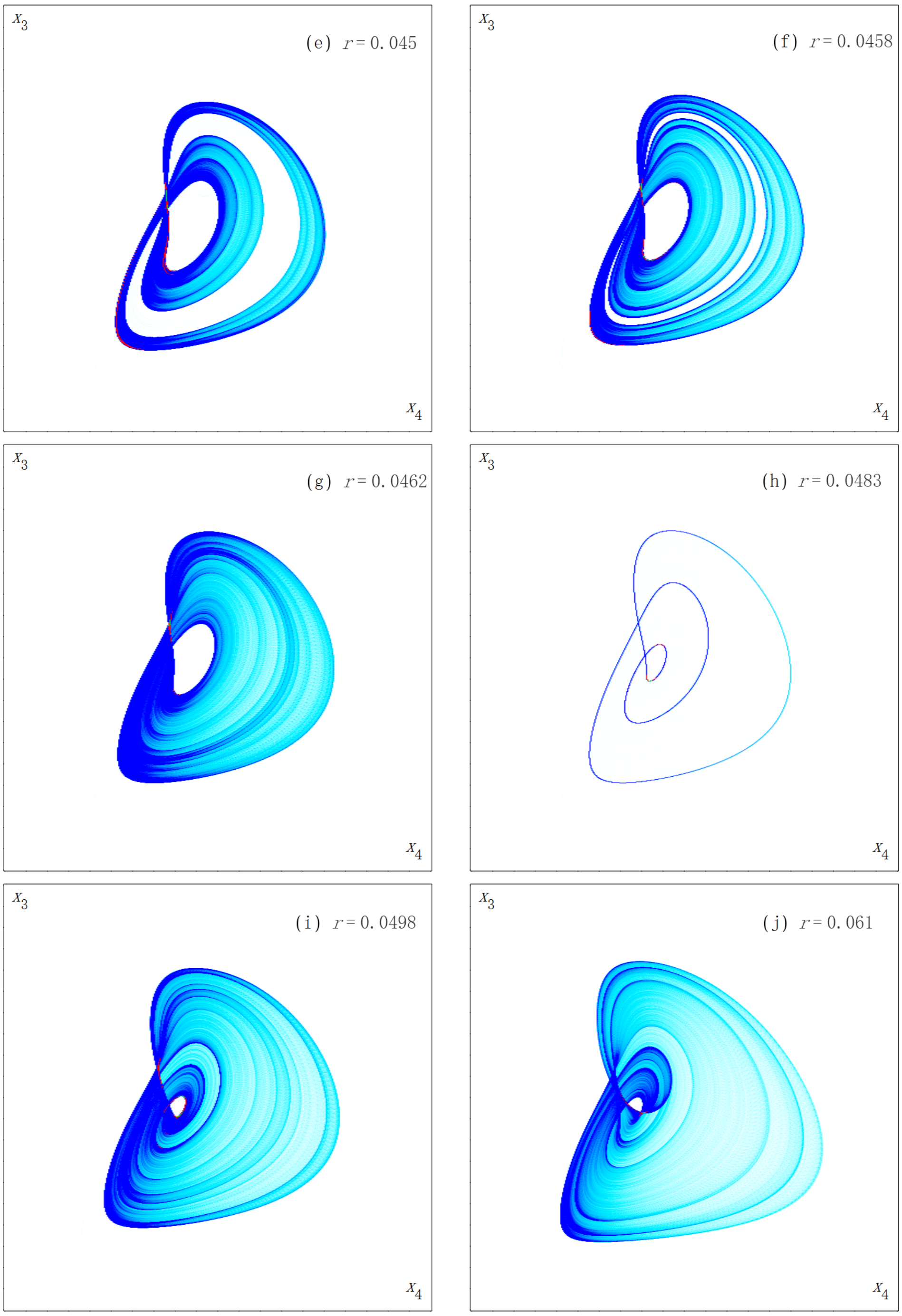

x_3
(e) $r = 0.045$
x_4
x_3
(f) $r = 0.0458$
x_4
x_3
(g) $r = 0.0462$
x_4
x_3
(h) $r = 0.0483$
x_4
x_3
(i) $r = 0.0498$
x_4
x_3
(j) $r = 0.061$
x_4

However, the story is not over. Another interesting finding is that the chaotic attractor disappears when $r = 0.112$, while a homoclinic connection occurs instead (Table 4(a)). A cascade of homoclinic-doubling bifurcation begins at about $r = 0.114$ (see Table 4(b)-(c) for the 2-homoclinic connection and 8-homoclinic connection), and leads to chaos finally (Table 4(d)-(e)). But then a homoclinic-halving cascade can also occur when $r > 0.131$, and the attractor turns into a homoclinic connection for $0.155 < r < 0.307$ (see Table 4(f)).

Table 4: Evolution of the attractor in the carrying simplex for system (29) as r increases from 0.112 to 0.156. Cascades of homoclinic-doubling bifurcations occur. The initial value used is $x_0 = (0.4, 0.3, 0.4, 0.5)$.

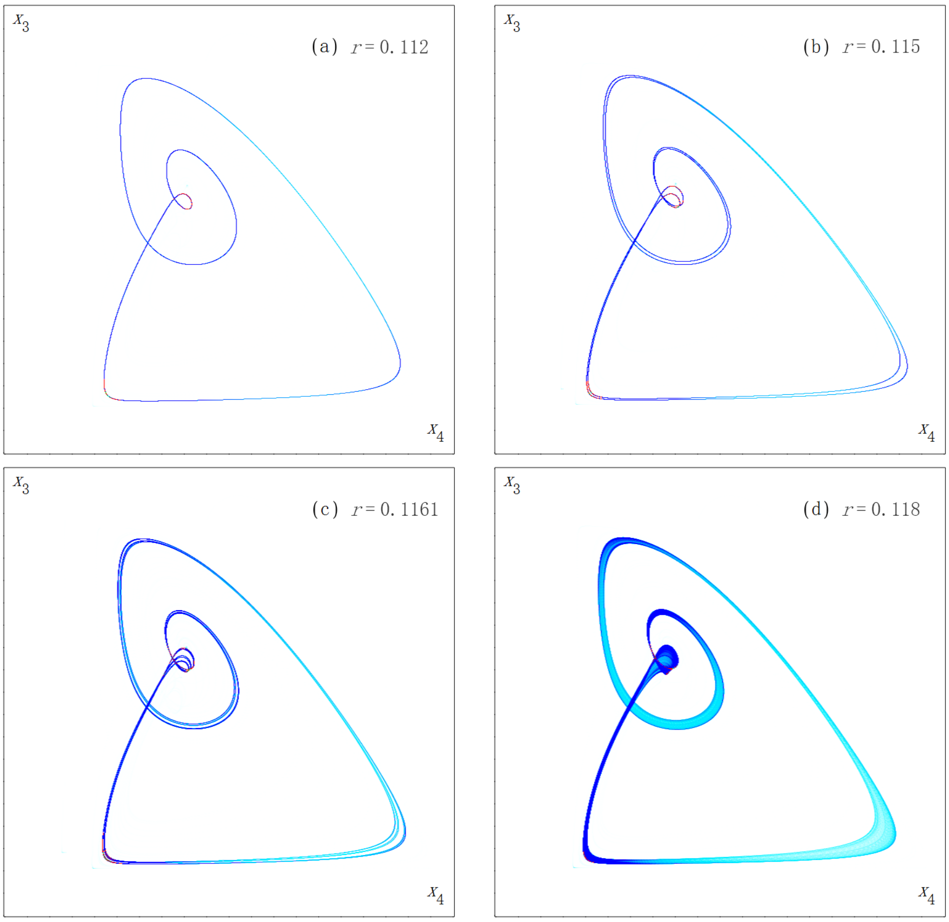

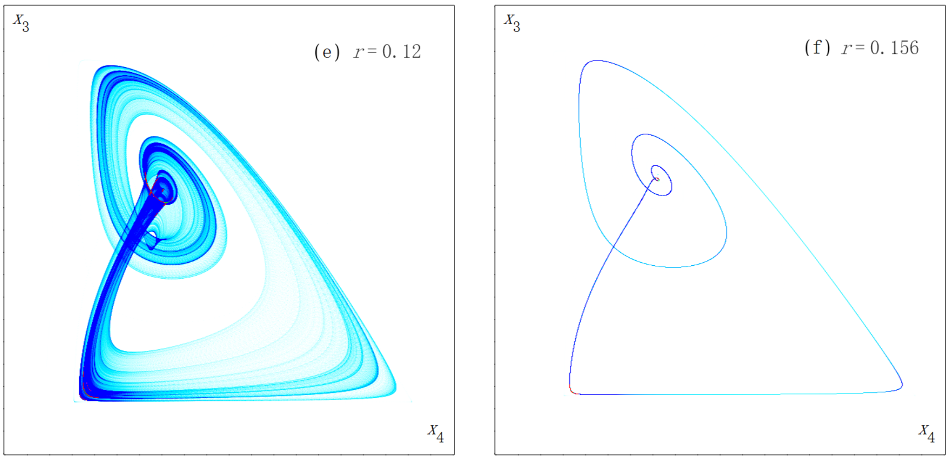

6. Discussion

The Ricker map (10) possesses a carrying simplex when the growth rates $\nu_i > 0$ are small, that is, when the basic reproduction ratios $R_0^{(i)}$ are close to 1. The carrying simplex captures the relevant long-term dynamics. Any 2D Rikcer model admitting a carrying simplex has trivial dynamics, that is, every orbit converges to some fixed point. An equivalence relation on the space CRC(3) of all 3D Ricker models (10) admitting a carrying simplex is defined, i.e., two such models are said to be equivalent if all the boundary fixed points have the same local dynamics on the carrying simplices after a permutation of the indices $\{1, 2, 3\}$. There are a total of 33 stable equivalence classes in CRC(3).

Specifically, in classes $1 - 18$, every nontrivial orbit converges to some fixed point on $\partial\Sigma$; in classes $19-25$, each map has a unique positive fixed point p which is a saddle on Σ, and every nontrivial orbit converges to some fixed point on $\partial\Sigma$, except those on the stable manifold of p; in class 33, the unique positive fixed point is globally asymptotically stable. The global dynamics of the maps from classes $1-25$ and 33 can be completely determined by the local dynamics of fixed points on $\partial\Sigma$. However, within each of classes $26-31$, there exist Neimark-Sacker bifurcations, and hence closed invariant curves can occur on the carrying simplex in these classes. Numerical experiments show that the 3D Ricker model possesses asymptotically attracting isolated quasiperiodic curves. Neimark-Sacker bifurcations do not occur in class 32. Class 29 can admit Chenciner bifurcations, so this class can admit two isolated closed invariant curves on the carrying simplex. Each map in class 27 has a heteroclinic cycle, i.e. a cyclic arrangement of saddle fixed points and heteroclinic connections. The competition coefficients in this class can be seen to correspond to the biological environment where in purely pairwise competition 1 beats 2, 2 beats 3, and 3 beats 1. It is this intransitivity in the pairwise competition which leads to such cyclic behavior. We further provide the criteria on the stability of heteroclinic cycles and construct systems which admit heteroclinic cycle attractors, i.e. the systems exhibit a general class of orbits which cycle from being composed almost wholly of species 1, to almost wholly 2, to almost wholly 3, back to almost wholly 1 etc ([47]).

One main advantage of our method is that we can give the classification of the dynamics via the boundary dynamics. The classification by the equivalence relative to the boundary dynamics (see Definition 2.1) for CRC(3) is also suitable for CRC(4) and higher dimensional Ricker maps. Since the dynamics has been studied for CRC(3), the boundary dynamics for each Ricker map in CRC(4) is known now. Therefore, it is possible to classify CRC(4) by the equivalence relation defined in Definition 2.1, and further to classify the higher dimensional Ricker maps. However, since we do not have an index formula like (20) for higher dimensional Ricker maps ($n \geq 4$), the classification program is much more complex than the 3D case, which is left as a future project.

It should be pointed out that when some ν_i is sufficiently large, the carrying simplex indeed breaks, and chaotic dynamics can appear. When some ν_i is sufficiently big, even the dynamics of species i becomes chaotic, and hence the carrying simplex breaks. For Ricker maps (10), at least three cascades of bifurcations can lead to chaos:

– cascades of period-doubling bifurcations lead to chaos;

– cascades of quasiperiod-doubling bifurcations lead to chaos;

– cascades of homoclinic-doubling bifurcations lead to chaos.

Cascades of period-doubling bifurcations may break the carrying simplex, while the other two cascades of bifurcations which lead to chaotic dynamics eventually, can occur in the carrying simplex. Such phenomena are numerically shown in detail by concrete examples; see Section 5.1 and Section 5.2.

It is worth noting that there are several problems remain open. We propose some as follows.

- Enlightened by Example 4.2, it is also an interesting problem to study how many closed invariant curves can coexist on the carrying simplex for 3D Ricker models.

- Whether the 3D Ricker model can possess a center on Σ or not is also unknown.

- Though there exist 4D Ricker models which admit a carrying simplex containing strange attractors, whether there exists a carrying simplex which contains a chaotic attractor for 3D Ricker models is unknown.

Acknowledgements

The authors are greatly indebted to two anonymous referees and the editor whose suggestions led to much improvement in the presentation of our results. The authors are also very grateful to Professor Saber Elaydi for the valuable discussion.

This work was supported by the National Natural Science Foundation of China (NSFC) under Grant No.11371252, Shanghai Gaofeng Project for University Academic Program Development, and the Academy of Finland.

Appendix A. The stable equivalence classes in CRC(3)

Table A.1: The 33 equivalence classes in CRC(3), where $\gamma_{ij} := \mu_{ii} - \mu_{ji}$, $\beta_{ij} = \frac{\mu_{jj}-\mu_{ij}}{\mu_{ii}\mu_{jj}-\mu_{ij}\mu_{ji}}$ for $i, j = 1, 2, 3$ and $i \neq j$, and each Σ is given by a representative map of that class. A fixed point is represented by a closed dot $\bullet$ if it attracts on Σ, by an open dot $\circ$ if it repels on Σ, and by the intersection of its hyperbolic manifolds if it is a saddle on Σ.

Class	Parameter conditions	Element	Phase Portrait
1	$\gamma_{12} < 0, \gamma_{13} < 0, \gamma_{21} > 0,$ $\gamma_{23} > 0, \gamma_{31} > 0, \gamma_{32} < 0$	$U = \begin{pmatrix} 1 & \frac{1}{2} & \frac{1}{2} \\ 2 & 1 & 2 \\ 2 & \frac{1}{2} & 1 \end{pmatrix}$ $\nu_1 = \frac{1}{3},\ \nu_2 = \frac{1}{6}$ $\nu_3 = \frac{1}{7}$	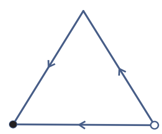
2	(i) $\gamma_{12} < 0, \gamma_{13} < 0, \gamma_{21} < 0,$ $\gamma_{23} > 0, \gamma_{31} > 0, \gamma_{32} < 0$ (ii) $u_{31}\beta_{12} + u_{32}\beta_{21} < 1$	$U = \begin{pmatrix} 1 & 3 & \frac{1}{3} \\ 3 & 1 & 3 \\ 3 & \frac{1}{3} & 1 \end{pmatrix}$ $\nu_1 = \frac{1}{5},\ \nu_2 = \frac{1}{8},$ $\nu_3 = \frac{1}{5}$	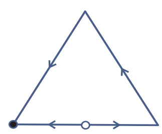

Table A.1: (continued)

Class	Parameter conditions	Element	Phase Portrait
3	(i) $\gamma_{12} < 0, \gamma_{13} < 0, \gamma_{21} > 0,$ $\gamma_{23} < 0, \gamma_{31} > 0, \gamma_{32} < 0$ (ii) $u_{12}\beta_{23} + u_{13}\beta_{32} < 1$	$U = \begin{pmatrix} 1 & \frac{1}{2} & \frac{1}{2} \\ 2 & 1 & 2 \\ 2 & 2 & 1 \end{pmatrix}$ $\nu_1 = \frac{1}{3},\ \nu_2 = \frac{1}{6},$ $\nu_3 = \frac{1}{6}$	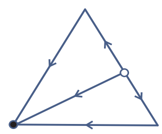
4	(i) $\gamma_{12} > 0, \gamma_{13} < 0, \gamma_{21} > 0,$ $\gamma_{23} < 0, \gamma_{31} > 0, \gamma_{32} < 0$ (ii) $u_{12}\beta_{23} + u_{13}\beta_{32} < 1$ (iii) $u_{31}\beta_{12} + u_{32}\beta_{21} > 1$	$U = \begin{pmatrix} 1 & \frac{1}{2} & \frac{1}{2} \\ \frac{1}{2} & 1 & 2 \\ 2 & 2 & 1 \end{pmatrix}$ $\nu_1 = \frac{1}{3},\ \nu_2 = \frac{1}{7},$ $\nu_3 = \frac{1}{6}$	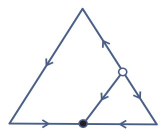
5	(i) $\gamma_{12} > 0, \gamma_{13} > 0, \gamma_{21} > 0,$ $\gamma_{23} < 0, \gamma_{31} < 0, \gamma_{32} > 0$ (ii) $u_{31}\beta_{12} + u_{32}\beta_{21} > 1$	$U = \begin{pmatrix} 1 & \frac{1}{2} & 2 \\ \frac{1}{2} & 1 & \frac{1}{2} \\ \frac{1}{2} & 2 & 1 \end{pmatrix}$ $\nu_1 = \frac{1}{7},\ \nu_2 = \frac{1}{3},$ $\nu_3 = \frac{1}{7}$	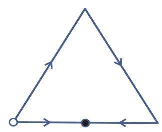
6	(i) $\gamma_{12} > 0, \gamma_{13} > 0, \gamma_{21} < 0,$ $\gamma_{23} > 0, \gamma_{31} < 0, \gamma_{32} > 0$ (ii) $u_{12}\beta_{23} + u_{13}\beta_{32} > 1$	$U = \begin{pmatrix} 1 & 2 & 2 \\ \frac{1}{2} & 1 & \frac{1}{2} \\ \frac{1}{2} & \frac{1}{2} & 1 \end{pmatrix}$ $\nu_1 = \frac{1}{6},\ \nu_2 = \frac{1}{3},$ $\nu_3 = \frac{1}{3}$	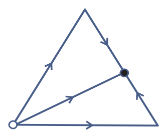
7	(i) $\gamma_{12} > 0, \gamma_{13} > 0, \gamma_{21} > 0,$ $\gamma_{23} > 0, \gamma_{31} < 0, \gamma_{32} < 0$ (ii) $u_{31}\beta_{12} + u_{32}\beta_{21} < 1$	$U = \begin{pmatrix} 1 & \frac{1}{3} & 3 \\ \frac{1}{3} & 1 & 3 \\ \frac{1}{3} & \frac{1}{3} & 1 \end{pmatrix}$ $\nu_1 = \frac{1}{5},\ \nu_2 = \frac{1}{5},$ $\nu_3 = \frac{1}{5}$	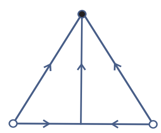
8	(i) $\gamma_{12} > 0, \gamma_{13} > 0, \gamma_{21} > 0,$ $\gamma_{23} < 0, \gamma_{31} < 0, \gamma_{32} < 0$ (ii) $u_{12}\beta_{23} + u_{13}\beta_{32} < 1$ (iii) $u_{31}\beta_{12} + u_{32}\beta_{21} < 1$	$U = \begin{pmatrix} 1 & \frac{1}{3} & \frac{4}{3} \\ \frac{2}{3} & 1 & \frac{4}{3} \\ \frac{1}{3} & \frac{4}{3} & 1 \end{pmatrix}$ $\nu_1 = \frac{1}{3},\ \nu_2 = \frac{1}{4},$ $\nu_3 = \frac{1}{3}$	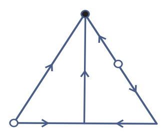
9	(i) $\gamma_{12} > 0, \gamma_{13} > 0, \gamma_{21} > 0,$ $\gamma_{23} > 0, \gamma_{31} < 0, \gamma_{32} > 0$ (ii) $u_{12}\beta_{23} + u_{13}\beta_{32} > 1$ (iii) $u_{31}\beta_{12} + u_{32}\beta_{21} < 1$	$U = \begin{pmatrix} 1 & \frac{1}{3} & 3 \\ \frac{1}{3} & 1 & \frac{1}{3} \\ \frac{1}{3} & \frac{1}{3} & 1 \end{pmatrix}$ $\nu_1 = \frac{1}{5},\ \nu_2 = \frac{2}{5},$ $\nu_3 = \frac{2}{5}$	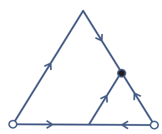

Table A.1: (continued)

Class	Parameter conditions	Element	Phase Portrait
10	(i) $\gamma_{12} > 0, \gamma_{13} > 0, \gamma_{21} > 0, \gamma_{23} > 0, \gamma_{31} < 0, \gamma_{32} > 0$ (ii) $u_{12}\beta_{23} + u_{13}\beta_{32} < 1$ (iii) $u_{31}\beta_{12} + u_{32}\beta_{21} > 1$	$U = \begin{pmatrix} 1 & \frac{1}{4} & \frac{5}{4} \\ \frac{1}{4} & 1 & \frac{1}{4} \\ \frac{3}{4} & \frac{3}{4} & 1 \end{pmatrix}$ $\nu_1 = \frac{1}{5},\ \nu_2 = \frac{1}{3},$ $\nu_3 = \frac{1}{5}$	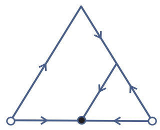
11	(i) $\gamma_{12} > 0, \gamma_{13} > 0, \gamma_{21} > 0, \gamma_{23} < 0, \gamma_{31} > 0, \gamma_{32} < 0$ (ii) $u_{12}\beta_{23} + u_{13}\beta_{32} < 1$ (iii) $u_{21}\beta_{13} + u_{23}\beta_{31} < 1$ (iv) $u_{31}\beta_{12} + u_{32}\beta_{21} > 1$	$U = \begin{pmatrix} 1 & \frac{1}{3} & \frac{1}{3} \\ \frac{1}{3} & 1 & \frac{4}{3} \\ \frac{2}{3} & 3 & 1 \end{pmatrix}$ $\nu_1 = \frac{2}{5},\ \nu_2 = \frac{1}{3},$ $\nu_3 = \frac{1}{5}$	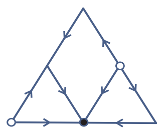
12	(i) $\gamma_{12} > 0, \gamma_{13} > 0, \gamma_{21} > 0, \gamma_{23} > 0, \gamma_{31} > 0, \gamma_{32} > 0$ (ii) $u_{12}\beta_{23} + u_{13}\beta_{32} < 1$ (iii) $u_{21}\beta_{13} + u_{23}\beta_{31} < 1$ (iv) $u_{31}\beta_{12} + u_{32}\beta_{21} > 1$	$U = \begin{pmatrix} 1 & \frac{1}{4} & \frac{1}{4} \\ \frac{1}{4} & 1 & \frac{1}{4} \\ \frac{3}{4} & \frac{3}{4} & 1 \end{pmatrix}$ $\nu_1 = \frac{1}{5},\ \nu_2 = \frac{1}{3},$ $\nu_3 = \frac{1}{3}$	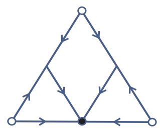
13	(i) $\gamma_{12} < 0, \gamma_{13} < 0, \gamma_{21} < 0, \gamma_{23} < 0, \gamma_{31} > 0, \gamma_{32} > 0$ (ii) $u_{31}\beta_{12} + u_{32}\beta_{21} > 1$	$U = \begin{pmatrix} \frac{1}{3} & 3 & 1 \\ \frac{1}{2} & 1 & 2 \\ 1 & 3 & 3 \end{pmatrix}$ $\nu_1 = \frac{1}{14},\ \nu_2 = \frac{1}{7},$ $\nu_3 = \frac{1}{7}$	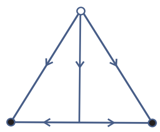
14	(i) $\gamma_{12} < 0, \gamma_{13} < 0, \gamma_{21} < 0, \gamma_{23} > 0, \gamma_{31} > 0, \gamma_{32} > 0$ (ii) $u_{12}\beta_{23} + u_{13}\beta_{32} > 1$ (iii) $u_{31}\beta_{12} + u_{32}\beta_{21} > 1$	$U = \begin{pmatrix} 1 & 2 & \frac{1}{2} \\ 2 & 1 & \frac{1}{2} \\ 4 & \frac{1}{2} & 1 \end{pmatrix}$ $\nu_1 = \frac{1}{7},\ \nu_2 = \frac{1}{7},$ $\nu_3 = \frac{1}{11}$	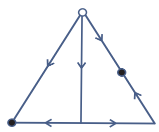
15	(i) $\gamma_{12} < 0, \gamma_{13} < 0, \gamma_{21} < 0, \gamma_{23} < 0, \gamma_{31} > 0, \gamma_{32} < 0$ (ii) $u_{12}\beta_{23} + u_{13}\beta_{32} < 1$ (iii) $u_{31}\beta_{12} + u_{32}\beta_{21} > 1$	$U = \begin{pmatrix} 1 & 2 & \frac{1}{2} \\ 2 & 1 & 2 \\ 2 & 2 & 1 \end{pmatrix}$ $\nu_1 = \frac{1}{7},\ \nu_2 = \frac{1}{6},$ $\nu_3 = \frac{1}{6}$	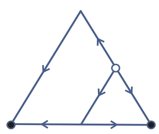

Table A.1: (continued)

Class	Parameter conditions	Element	Phase Portrait
16	(i) $\gamma_{12} < 0, \gamma_{13} < 0, \gamma_{21} < 0,$ $\gamma_{23} < 0, \gamma_{31} > 0, \gamma_{32} < 0$ (ii) $u_{12}\beta_{23} + u_{13}\beta_{32} > 1$ (iii) $u_{31}\beta_{12} + u_{32}\beta_{21} < 1$	$U = \begin{pmatrix} 1 & 3 & \frac{1}{3} \\ 3 & 1 & 3 \\ \frac{3}{2} & \frac{3}{2} & 1 \end{pmatrix}$ $\nu_1 = \frac{1}{5},\ \ \nu_2 = \frac{1}{8},$ $\nu_3 = \frac{1}{5}$	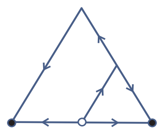
17	(i) $\gamma_{12} < 0, \gamma_{13} < 0, \gamma_{21} < 0,$ $\gamma_{23} > 0, \gamma_{31} < 0, \gamma_{32} > 0$ (ii) $u_{12}\beta_{23} + u_{13}\beta_{32} > 1$ (iii) $u_{21}\beta_{13} + u_{23}\beta_{31} > 1$ (iv) $u_{31}\beta_{12} + u_{32}\beta_{21} < 1$	$U = \begin{pmatrix} 1 & 2 & 2 \\ 4 & 1 & \frac{1}{2} \\ 2 & \frac{1}{2} & 1 \end{pmatrix}$ $\nu_1 = \frac{1}{6},\ \ \nu_2 = \frac{1}{11},$ $\nu_3 = \frac{1}{7}$	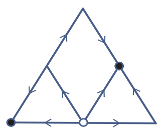
18	(i) $\gamma_{12} < 0, \gamma_{13} < 0, \gamma_{21} < 0,$ $\gamma_{23} < 0, \gamma_{31} < 0, \gamma_{32} < 0$ (ii) $u_{12}\beta_{23} + u_{13}\beta_{32} > 1$ (iii) $u_{21}\beta_{13} + u_{23}\beta_{31} > 1$ (iv) $u_{31}\beta_{12} + u_{32}\beta_{21} < 1$	$U = \begin{pmatrix} 1 & 3 & 3 \\ 3 & 1 & 3 \\ \frac{3}{2} & \frac{3}{2} & 1 \end{pmatrix}$ $\nu_1 = \frac{1}{8},\ \ \nu_2 = \frac{1}{8},$ $\nu_3 = \frac{1}{5}$	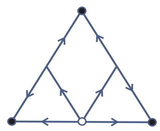
19	(i) $\gamma_{12} > 0, \gamma_{13} > 0, \gamma_{21} < 0,$ $\gamma_{23} < 0, \gamma_{31} < 0, \gamma_{32} < 0$ (ii) $u_{12}\beta_{23} + u_{13}\beta_{32} < 1$	$U = \begin{pmatrix} 1 & \frac{3}{2} & \frac{3}{2} \\ \frac{1}{3} & 1 & 3 \\ \frac{1}{3} & 3 & 1 \end{pmatrix}$ $\nu_1 = \frac{1}{5},\ \ \nu_2 = \frac{1}{5},$ $\nu_3 = \frac{1}{5}$	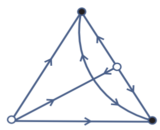
20	(i) $\gamma_{12} < 0, \gamma_{13} < 0, \gamma_{21} < 0,$ $\gamma_{23} < 0, \gamma_{31} > 0, \gamma_{32} < 0$ (ii) $u_{12}\beta_{23} + u_{13}\beta_{32} < 1$ (iii) $u_{31}\beta_{12} + u_{32}\beta_{21} < 1$	$U = \begin{pmatrix} 1 & \frac{5}{3} & \frac{1}{3} \\ 3 & 1 & \frac{4}{3} \\ \frac{4}{3} & \frac{4}{3} & 1 \end{pmatrix}$ $\nu_1 = \frac{1}{4},\ \ \nu_2 = \frac{1}{8},$ $\nu_3 = \frac{1}{4}$	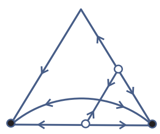
21	(i) $\gamma_{12} < 0, \gamma_{13} < 0, \gamma_{21} < 0,$ $\gamma_{23} > 0, \gamma_{31} < 0, \gamma_{32} > 0$ (ii) $u_{12}\beta_{23} + u_{13}\beta_{32} > 1$ (iii) $u_{21}\beta_{13} + u_{23}\beta_{31} < 1$ (iv) $u_{31}\beta_{12} + u_{32}\beta_{21} < 1$	$U = \begin{pmatrix} 1 & 2 & 2 \\ 2 & 1 & \frac{1}{2} \\ 2 & \frac{1}{2} & 1 \end{pmatrix}$ $\nu_1 = \frac{1}{6},\ \ \nu_2 = \frac{1}{7},$ $\nu_3 = \frac{1}{7}$	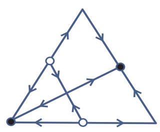

Table A.1: (continued)

Class	Parameter conditions	Element	Phase Portrait
22	(i) $\gamma_{12} > 0, \gamma_{13} > 0, \gamma_{21} < 0,$ $\gamma_{23} < 0, \gamma_{31} > 0, \gamma_{32} < 0$ (ii) $u_{12}\beta_{23} + u_{13}\beta_{32} < 1$ (iii) $u_{21}\beta_{13} + u_{23}\beta_{31} > 1$	$U = \begin{pmatrix} 1 & 2 & \frac{1}{2} \\ \frac{1}{2} & 1 & 2 \\ \frac{1}{2} & 2 & 1 \end{pmatrix}$ $\nu_1 = \frac{1}{7},\ \nu_2 = \frac{1}{7},$ $\nu_3 = \frac{1}{7}$	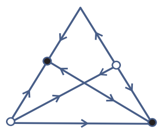
23	(i) $\gamma_{12} > 0, \gamma_{13} > 0, \gamma_{21} > 0,$ $\gamma_{23} > 0, \gamma_{31} < 0, \gamma_{32} < 0$ (ii) $u_{31}\beta_{12} + u_{32}\beta_{21} > 1$	$U = \begin{pmatrix} 1 & \frac{1}{4} & 4 \\ \frac{1}{4} & 1 & 4 \\ \frac{3}{4} & \frac{3}{4} & 1 \end{pmatrix}$ $\nu_1 = \frac{1}{6},\ \nu_2 = \frac{1}{6},$ $\nu_3 = \frac{1}{5}$	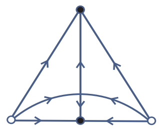
24	(i) $\gamma_{12} > 0, \gamma_{13} > 0, \gamma_{21} > 0,$ $\gamma_{23} > 0, \gamma_{31} < 0, \gamma_{32} > 0$ (ii) $u_{12}\beta_{23} + u_{13}\beta_{32} > 1$ (iii) $u_{31}\beta_{12} + u_{32}\beta_{21} > 1$	$U = \begin{pmatrix} 1 & \frac{1}{4} & \frac{25}{4} \\ \frac{1}{4} & 1 & \frac{1}{4} \\ \frac{3}{4} & \frac{5}{8} & 1 \end{pmatrix}$ $\nu_1 = \frac{1}{8},\ \nu_2 = \frac{1}{3},$ $\nu_3 = \frac{1}{3}$	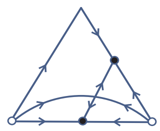
25	(i) $\gamma_{12} > 0, \gamma_{13} > 0, \gamma_{21} > 0,$ $\gamma_{23} < 0, \gamma_{31} > 0, \gamma_{32} < 0$ (ii) $u_{12}\beta_{23} + u_{13}\beta_{32} < 1$ (iii) $u_{21}\beta_{13} + u_{23}\beta_{31} > 1$ (iv) $u_{31}\beta_{12} + u_{32}\beta_{21} > 1$	$U = \begin{pmatrix} 1 & \frac{1}{2} & \frac{1}{2} \\ \frac{1}{2} & 1 & 2 \\ \frac{1}{2} & 2 & 1 \end{pmatrix}$ $\nu_1 = \frac{1}{3},\ \nu_2 = \frac{1}{7},$ $\nu_3 = \frac{1}{7}$	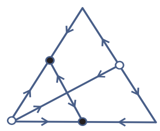
26	(i) $\gamma_{12} > 0, \gamma_{13} > 0, \gamma_{21} < 0,$ $\gamma_{23} < 0, \gamma_{31} > 0, \gamma_{32} < 0$ (ii) $u_{12}\beta_{23} + u_{13}\beta_{32} > 1$ (iii) $u_{21}\beta_{13} + u_{23}\beta_{31} < 1$	$U = \begin{pmatrix} 1 & 4 & \frac{3}{4} \\ \frac{1}{4} & 1 & \frac{5}{4} \\ \frac{3}{4} & \frac{5}{4} & 1 \end{pmatrix}$ $\nu_1 = \frac{1}{6},\ \nu_2 = \frac{1}{5},$ $\nu_3 = \frac{1}{4}$	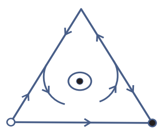
27	$\gamma_{12} > 0, \gamma_{13} < 0, \gamma_{21} < 0,$ $\gamma_{23} > 0, \gamma_{31} > 0, \gamma_{32} < 0$	$U = \begin{pmatrix} 1 & 2 & \frac{1}{2} \\ \frac{1}{2} & 1 & 2 \\ 2 & \frac{1}{2} & 1 \end{pmatrix}$ $\nu_1 = \frac{1}{7},\ \nu_2 = \frac{1}{7},$ $\nu_3 = \frac{1}{7}$	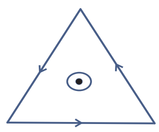
28	(i) $\gamma_{12} < 0, \gamma_{13} < 0, \gamma_{21} < 0,$ $\gamma_{23} > 0, \gamma_{31} > 0, \gamma_{32} < 0$ (ii) $u_{31}\beta_{12} + u_{32}\beta_{21} > 1$	$U = \begin{pmatrix} 1 & \frac{3}{2} & \frac{3}{4} \\ 2 & 1 & 2 \\ 4 & \frac{1}{2} & 1 \end{pmatrix}$ $\nu_1 = \frac{1}{4},\ \nu_2 = \frac{1}{6},$ $\nu_3 = \frac{1}{11}$	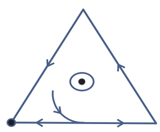

Table A.1: (continued)

Class	Parameter conditions	Element	Phase Portrait
29	(i) $\gamma_{12} > 0, \gamma_{13} > 0, \gamma_{21} > 0,$ $\gamma_{23} < 0, \gamma_{31} < 0, \gamma_{32} > 0$ (ii) $u_{31}\beta_{12} + u_{32}\beta_{21} < 1$	$U = \begin{pmatrix} 1 & \frac{1}{2} & 2 \\ \frac{1}{2} & 1 & \frac{1}{2} \\ \frac{1}{6} & \frac{7}{6} & 1 \end{pmatrix}$ $\nu_1 = \frac{1}{7},\ \ \nu_2 = \frac{1}{3},$ $\nu_3 = \frac{2}{7}$	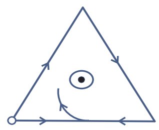
30	(i) $\gamma_{12} < 0, \gamma_{13} < 0, \gamma_{21} < 0,$ $\gamma_{23} < 0, \gamma_{31} > 0, \gamma_{32} < 0$ (ii) $u_{12}\beta_{23} + u_{13}\beta_{32} > 1$ (iii) $u_{31}\beta_{12} + u_{32}\beta_{21} > 1$	$U = \begin{pmatrix} 1 & 4 & \frac{1}{2} \\ 2 & 1 & 2 \\ 2 & 2 & 1 \end{pmatrix}$ $\nu_1 = \frac{1}{11},\ \ \nu_2 = \frac{1}{6},$ $\nu_3 = \frac{1}{6}$	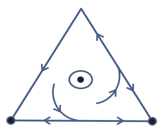
31	(i) $\gamma_{12} > 0, \gamma_{13} > 0, \gamma_{21} > 0,$ $\gamma_{23} > 0, \gamma_{31} < 0, \gamma_{32} > 0$ (ii) $u_{12}\beta_{23} + u_{13}\beta_{32} < 1$ (iii) $u_{31}\beta_{12} + u_{32}\beta_{21} < 1$	$U = \begin{pmatrix} 1 & \frac{1}{4} & \frac{5}{4} \\ \frac{5}{8} & 1 & \frac{5}{8} \\ \frac{1}{4} & \frac{3}{4} & 1 \end{pmatrix}$ $\nu_1 = \frac{1}{5},\ \ \nu_2 = \frac{1}{3},$ $\nu_3 = \frac{1}{3}$	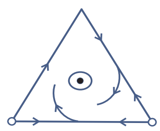
32	(i) $\gamma_{12} < 0, \gamma_{13} < 0, \gamma_{21} < 0,$ $\gamma_{23} < 0, \gamma_{31} < 0, \gamma_{32} < 0$ (ii) $u_{12}\beta_{23} + u_{13}\beta_{32} > 1$ (iii) $u_{21}\beta_{13} + u_{23}\beta_{31} > 1$ (iv) $u_{31}\beta_{12} + u_{32}\beta_{21} > 1$	$U = \begin{pmatrix} 1 & 2 & 2 \\ 2 & 1 & 2 \\ 2 & 2 & 1 \end{pmatrix}$ $\nu_1 = \frac{1}{6},\ \ \nu_2 = \frac{1}{6},$ $\nu_3 = \frac{1}{6}$	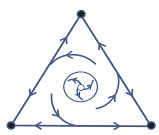
33	(i) $\gamma_{12} > 0, \gamma_{13} > 0, \gamma_{21} > 0,$ $\gamma_{23} > 0, \gamma_{31} > 0, \gamma_{32} > 0$ (ii) $u_{12}\beta_{23} + u_{13}\beta_{32} < 1$ (iii) $u_{21}\beta_{13} + u_{23}\beta_{31} < 1$ (iv) $u_{31}\beta_{12} + u_{32}\beta_{21} < 1$	$U = \begin{pmatrix} 1 & \frac{1}{2} & \frac{1}{2} \\ \frac{1}{2} & 1 & \frac{1}{2} \\ \frac{1}{2} & \frac{1}{2} & 1 \end{pmatrix}$ $\nu_1 = \frac{1}{3},\ \ \nu_2 = \frac{1}{3},$ $\nu_3 = \frac{1}{3}$	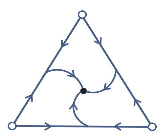

References

[1] A. S. Ackleh, P. L. Salceanu, Competitive exclusion and coexistence in an n-species Ricker model, J. Biol. Dyn. 9 (2015) 321–331.

[2] S. Baigent, Convexity-preserving flows of totally competitive planar Lotka–Volterra equations and the geometry of the carrying simplex, Proc. Edinb. Math. Soc. 55 (2012) 53–63.

[3] S. Baigent, Geometry of carrying simplices of 3-species competitive Lotka–Volterra systems, Nonlinearity 26 (2013) 1001–1029.
[4] S. Baigent, Convexity of the carrying simplex for discrete-time planar competitive Kolmogorov systems, J. Difference Equ. Appl. 22 (2016) 609–622.
[5] S. Baigent, Z. Hou, Global stability of interior and boundary fixed points for Lotka–Volterra systems, Differ. Equ. Dyn. Syst. 20 (2012) 53–66.
[6] E. C. Balreira, S. Elaydi, R. Luís, Local stability implies global stability for the planar Ricker competition model, Discret. Contin. Dyn. Syst. Ser. B 19 (2014) 323–351.
[7] F. A. Bartha, A. Garab, T. Krisztin, Local stability implies global stability for the 2-dimensional Ricker map, J. Difference Equ. Appl. 19 (2013) 2043–2078.
[8] X. Chen, J. Jiang, L. Niu, On Lotka–Volterra equations with identical minimal intrinsic growth rate, SIAM J. Applied Dyn. Sys. 14 (2015) 1558–1599.
[9] J. M. Cushing, On the fundamental bifurcation theorem for semelparous Leslie models, Chapter 11 in Mathematics of Planet Earth: Dynamics, Games and Science, J. P. Bourguignon, R. Jeltsch, A. Pinto, and M. Viana, eds, CIM Mathematical Sciences Series, Springer, Berlin, 2015 .
[10] N. V. Davydova, O. Diekmann, S. A. van Gils, On circulant populations. I. The algebra of semelparity, J. Lin. Algebra and Applications 398 (2005) 185–243.
[11] O. Diekmann, Y. Wang, P. Yan, Carrying simplices in discrete competitive systems and age-structured semelparous populations, Discrete Contin. Dyn. Syst. 20 (2008) 37–52.
[12] L. Gardini, R. Lupini, C. Mammana, M. G. Messia, Bifurcations and transitions to chaos in the three-dimensional Lotka–Volterra map, SIAM J. Appl. Math. 47 (1987) 455–482.
[13] A. Gaunersdorfer, C. H. Hommes, F. O. O. Wagener, Bifurcation routes to volatility clustering under evolutionary learning, Journal of Economic Behavior & Organization 67 (2008) 27–47.
[14] S. A. H. Geritz, Resident-invader dynamics and the coexistence of similar strategies, J. Math. Biol. 50 (2005) 67–82.
[15] S. A. H. Geritz, M. Gyllenberg, F. J. A. Jacobs, K. Parvinen, Invasion dynamics and attractor inheritance, J. Math. Biol. 44 (2002) 548–560.
[16] S. A. H. Geritz, E. Kisdi, G. Meszéna, J. A. J. Metz, Evolutionarily singular strategies and the adaptive growth and branching of the evolutionary tree, Evolutionary Ecology 12 (1998) 35–57.
[17] S. A. H. Geritz, J. A. J. Metz, E. Kisdi, G. Meszéna, Dynamics of adaptation and evolutionary branching, Phys. Rev. Letters 78 (1997) 2024–2027.
[18] W. Govaerts, R. K. Ghaziani, Y. A. Kuznetsov, H. G. E. Meijer, Numerical methods for two-parameter local bifurcation analysis of maps, SIAM J. Sci. Comput. 29 (2007) 2644–2667.
[19] W. Govaerts, Y. A. Kuznetsov, H. G. E. Meijer, N. Neirynck, A study of resonance tongues near a Chenciner bifurcation using MatcontM, in: European Nonlinear Dynamics Conference, 24–29, 2011.
[20] M. Gyllenberg, J. Jiang, L. Niu, A note on global stability of three-dimensional Ricker models, J. Difference Equ. Appl. 25 (2019) 142–150.
[21] M. Gyllenberg, P. Yan, Four limit cycles for a three-dimensional competitive Lotka–Volterra system with a heteroclinic cycle, Comp. Math. Appl. 58 (2009) 649–669.
[22] M. Gyllenberg, P. Yan, On the number of limit cycles for three dimensional Lotka–Volterra systems, Discrete Contin. Dyn. Syst. Ser. B 11 (2009) 347–352.
[23] M. Gyllenberg, P. Yan, Y. Wang, A 3D competitive Lotka-Volterra system with three limit cycles: A falsification of a conjecture by Hofbauer and So, Appl. Math. Lett. 19 (2006) 1–7.
[24] M. W. Hirsch, Systems of differential equations which are competitive or cooperative: III. Competing species, Nonlinearity 1 (1988) 51–71.
[25] M. W. Hirsch, On existence and uniqueness of the carrying simplex for competitive dy-

namical systems, J. Biol. Dyn. 2 (2008) 169–179.
[26] J. Hofbauer, V. Hutson, W. Jansen, Coexistence for systems governed by difference equations of Lotka–Volterra type, J. Math. Biol. 25 (1987) 553–570.
[27] J. Hofbauer, K. Sigmund, Evolutionary Games and Population Dynamics, Cambridge University Press, Cambridge, 1998.
[28] J. Hofbauer, J. W.-H. So, Multiple limit cycles for three dimensional Lotka–Volterra equations, Appl. Math. Lett. 7 (1994) 65–70.
[29] Z. Hou, S. Baigent, Fixed point global attractors and repellors in competitive Lotka–Volterra systems, Dyn. Syst. 26 (2011) 367–390.
[30] Z. Hou, S. Baigent, Global stability and repulsion in autonomous Kolmogorov systems, Commun. Pure Appl. Anal. 14 (2015) 1205–1238.
[31] H. Jiang, T. D. Rogers, The discrete dynamics of symmetric competition in the plane, J. Math. Biol. 25 (1987) 573–596.
[32] J. Jiang, L. Niu, On the equivalent classification of three-dimensional competitive Atkinson/Allen models relative to the boundary fixed points, Discrete Contin. Dyn. Syst. 36 (2016) 217–244.
[33] J. Jiang, L. Niu, On the equivalent classification of three-dimensional competitive Leslie/Gower models via the boundary dynamics on the carrying simplex, J. Math. Biol. 74 (2017) 1223–1261.
[34] J. Jiang, L. Niu, Y. Wang, On heteroclinic cycles of competitive maps via carrying simplices, J. Math. Biol. 72 (2016) 939–972.
[35] J. Jiang, L. Niu, D. Zhu, On the complete classification of nullcline stable competitive three-dimensional Gompertz models, Nonlinear Anal. R.W.A. 20 (2014) 21–35.
[36] M. Kisaka, H. Kokubu, H. Oka, Supplement to homoclinic doubling bifurcation in vector fields, in Dynamical Systems, R. Bamon, J. Labarca, J. Lewowicz and J. Palis, eds., Longman, London (1993) 92–116.
[37] Y. A. Kuznetsov, Elements of applied bifurcation theory, second edition, Springer-Verlag, New York, 1998.
[38] Y. A. Kuznetsov, R. J. Sacker, Neimark-Sacker bifurcation, Scholarpedia 3 (2008) 1845.
[39] Z. Lu, Y. Luo, Three limit cycles for a three-dimensional Lotka–Volterra competitive system with a heteroclinic cycle, Comp. Math. Appl. 46 (2003) 231–238.
[40] R. Luís, S. Elaydi, H. Oliveira, Stability of a Ricker-type competition model and the competitive exclusion principle, J. Biol. Dyn. 5 (2011) 636–660.
[41] R. M. May, G. F. Oster, Bifurcations and dynamic complexity in simple ecological models, Am. Nat. 110 (1976) 573–599.
[42] J. Mierczyński, The C^1-property of carrying simplices for a class of competitive systems of ODEs, J. Differential Equations 111 (1994) 385–409.
[43] J. Mierczyński, L. Niu, A. Ruiz-Herrera, Linearization and invariant manifolds on the carrying simplex for competitive maps, J. Differential Equations (2019), https://doi.org/10.1016/j.jde.2019.08.001 .
[44] L. Niu, A. Ruiz-Herrera, Trivial dynamics in discrete-time systems: carrying simplex and translation arcs, Nonlinearity 31 (2018) 2633–2650.
[45] W. E. Ricker, Stock and recruitment, J. Fish. Res. Board. Can. 11 (1954) 559–623.
[46] L.-I. W. Roeger, Discrete May–Leonard competition models II, Discret. Contin. Dyn. Syst. Ser. B 5 (2005) 841–860.
[47] L.-I. W. Roeger, L. J. S. Allen, Discrete May-Leonard competition models I, J. Diff. Equ. Appl. 10 (2004) 77–98.
[48] O. E. Rössler, An equation for continuous chaos, Phys. Lett. A 57 (1976) 397–398.
[49] A. Ruiz-Herrera, Exclusion and dominance in discrete population models via the carrying simplex, J. Diff. Equ. Appl. 19 (2013) 96–113.
[50] B. Ryals, R. J. Sacker, Global stability in the 2D Ricker equation, J. Difference Equ. Appl.

21 (2015) 1068–1081.
[51] B. Ryals, R. J. Sacker, Global stability in the 2D Ricker equation revisited, Discret. Contin. Dyn. Syst. Ser. B 22 (2016) 585–604.
[52] H. L. Smith, Periodic competitive differential equations and the discrete dynamics of competitive maps, J. Differential Equations 64 (1986) 165–194.
[53] H. L. Smith, Planar competitive and cooperative difference equations, J. Diff. Equ. Appl. 3 (1998) 335–357.
[54] P. van den Driessche, M. L. Zeeman, Three-dimensional competitive Lotka–Volterra systems with no periodic orbits, SIAM J. Appl. Math. 58 (1998) 227–234.
[55] L. van Veen, The quasi-periodic doubling cascade in the transition to weak turbulence, Phys. D 210 (2005) 249–261.
[56] Y. Wang, J. Jiang, Uniqueness and attractivity of the carrying simplex for discrete-time competitive dynamical systems, J. Differential Equations 186 (2002) 611–632.
[57] D. Xiao, W. Li, Limit cycles for the competitive three dimensional Lotka–Volterra system, J. Differential Equations 164 (2000) 1–15.
[58] P. Yu, M. Han, D. Xiao, Four small limit cycles around a Hopf singular point in 3-dimensional competitive Lotka–Volterra systems, J. Math. Anal. Appl. 436 (2016) 521–555.
[59] E. C. Zeeman, M. L. Zeeman, On the convexity of carrying simplices in competitive Lotka–Volterra systems, in Differential Equations, Dynamical Systems, and Control Science, Lecture Notes in Pure and Appl. Math., 152, Dekker, New York (1994) 353–364.
[60] E. C. Zeeman, M. L. Zeeman, From local to global behavior in competitive Lotka–Volterra systems, Trans. Amer. Math. Soc. 355 (2002) 713–734.
[61] E. C. Zeeman, M. L. Zeeman, An n-dimensional competitive Lotka–Volterra system is generically determined by the edges of its carrying simplex, Nonlinearity 15 (2002) 2019–2032.
[62] M. L. Zeeman, Hopf bifurcations in competitive three-dimensional Lotka–Volterra systems, Dynam. Stability Systems 8 (1993) 189–217.